Electronic Supplementary Material (ESI) for New Journal of Chemistry.

Manuscript ID:

Manuscript title: van der Waals Interactions for Controlling Amide *cis-trans* Isomerism

Authors: Sunil K. Gupta, Shreya Banerjee, Erode N. Prabhakaran*

Affiliation: Department of Organic Chemistry, Indian Institute of Science, Bangalore, Karnataka - 560012, India.

E-mail: eprabhak@iisc.ac.in; erodeprabhakaran02@gmail.com.

Tel.: +91 80 2293 3380; Fax: (+) 91 80 2360 0529

Table of Contents **Page No.**

S1. Materials

All the reactions were performed in oven dried apparatus and were stirred using magnetic stir-bars. Column chromatography was performed on silica gel (100-200 mess) (Acme's) purchased from Sd-fine chemicals. Thin Layer Chromatography (TLC) was carried out on Merck DC Kieselgel 60 F254 aluminium sheets. Compounds were visualized by one of the (or all of the) following methods: (1) fluorescence quenching, (2) spray with a 0.2% (w/v) ninhydrin solution in absolute ethanol, (3) spray with 1% H_2SO_4 solution in EtOH/H_2O (1:5 v/v), (4) charring on hot plate. Ethylacetate and hexanes (or low boiling fractions of petroleum ether) were obtained from Sd-fine chemicals and were fractionally distilled at their respective boiling points, before use. Dichloromethane was dried by distillation over phosphorus pentoxide (P_2O_5). N-methyl Morpholine (NMM) was distilled over calcium hydride (CaH_2). NMR spectra were recorded on BRUKER-AV400 (400 MHz) spectrometer (Bruker Co., Faellanden, Switzerland). Chemical shifts are expressed in parts per million (ppm) from the residual non-deuterated chloroform in $CDCl_3$ (δ_H = 7.26 ppm, δ_C = 77.00 ppm). *J* values are expressed in Hertz (Hz). Multiplicities are indicated using the following abbreviations: s (singlet), d (doublet), dd (doublet of doublets), dt (doublet of triplet), t (triplet), q (quartet), quin (quintet), sext (sextet), hept (heptet), m (multiplet), bs (broad singlet). 2D NMR spectra were recorded in phase sensitive mode using time-proportional phase incrementation for quadrature detection in the t_1 dimension. Mass spectra were obtained with Micromass Q-Tof (ESI-HRMS). Melting points analyses were performed in VEEGO melting point apparatus (VEEGO Inst. Co., Mumbai, India).

S2. Methods

S2.1. HSQC Experiment:

The HSQC spectra were recorded at 300 K with a mixing time of 200 ms using the hsqctgpsi2 pulse sequence. An HSQC continuous wave spin-lock of 1.5 KHz was used to collect 2K points in the *f2* domain and 512 points in the *f1* domain. The data were processed using Bruker TOPSPIN 3.0 version software.

S2.2. TOCSY Experiment:

The TOCSY spectra were recorded at 300 K with mixing time of 200 ms using the MLEVPH pulse sequence. A TOCSY continuous wave spin-lock of 1.5 KHz was used to collect 2K points

in the *f2* domain and 512 points in the *f1* domain. The data were processed using Bruker TOPSPIN 3.0 version software. A 90^{o} sine-squared window function was applied in both directions.

S2.3. ROESY Experiment:

The ROESY spectra were recorded at 300 K with mixing time of 300 ms using ROESYPH pulse sequence. A ROESY continuous wave spin-lock of 1.5 KHz was used to collect 2K points in the *f2* domain and 512 points in the *f1* domain. The data were processed using Bruker TOPSPIN 3.0 version software. A 90^{o} sine-squared window function was applied in both directions.

S2.4 Crystal Structure Determination

Single crystals of the peptide **2** was obtained by slow evaporation of solvent from a solution in a mixture of ethylacetate : hexane (1:2). X-ray diffraction data were collected at -173 °C on a Brucker KAPPA APEX2 diffractometer using Mo K_{α} radiation. The data were collected using multi-scan mode. The structure was obtained by using direct methods in SHELXD[1] and was refined against F_2 by the full matrix least squares method using SHELXL-97.[2] Hydrogen atoms were fixed geometrically in idealized positions and were refined as riding over the heavy atoms to which they are bonded. The crystal and diffraction parameters are provided separately. **CCDC 994103** contains the supplementary crystallographic data for this paper. This data can be obtained free of charge via www.ccdc.cam. ac.uk/conts/retrieving.html (or from the Cambridge Crystallographic Data Centre, 12 Union Road, Cambridge CB21EZ, UK; fax: (+44) 1223-336-033; or e-mail: deposit@ccdc.cam.ac.uk).

1. Schneider, T. R.; Sheldrick, G. M., Substructure solution with SHELXD. *Acta Crystallographica Section D* **2002,** *58* (10 Part 2), 1772-1779.

2. Sheldrick, G. M. SHELXL-97, A Program for Crystal Structure Refinement; University of Gottingen: Gottingen, 1997.

S3. NMR markers for C-H…π interactions at Pro-Pro-Xaa motifs when Xaa = aromatic

Figure 1.

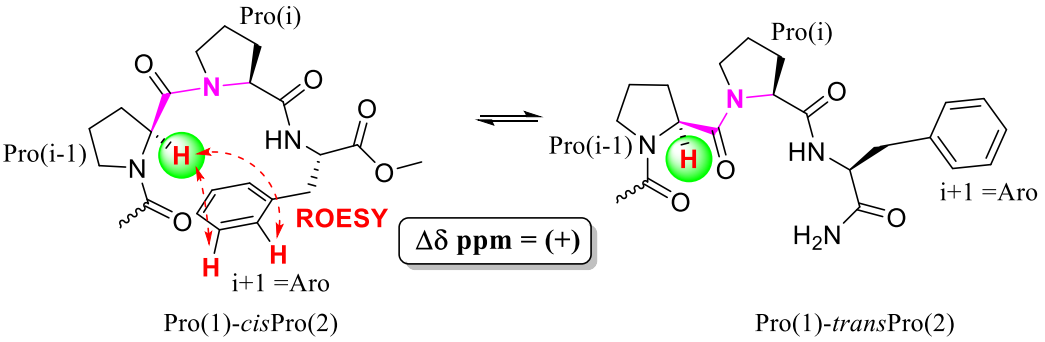

$\Delta\delta_{ppm}$ = Δδ(trans-cis) ppm = δ ($H^{\alpha}_{Pro(i-1)}$ in *trans*Pro rotamer) - δ ($H^{\alpha}_{Pro(i-1)}$ in *cis*Pro rotamer)

Neither ROESY nor Δδ is observed when i+1 = Alp

Reference: Ganguly, H. K.; Majumder, B.; Chattopadhyay, S.; Chakrabarti, P.; Basu, G., Direct Evidence for CH···π Interaction Mediated Stabilization of Pro-cisPro Bond in Peptides with Pro-Pro-Aromatic motifs. *J. Am. Chem. Soc.* **2012,** *134* (10), 4661-4669.

S4. Crystal structure of Ibu-*cis*Pro-Val-OMe (2) (Ibu = isobutyroyl)

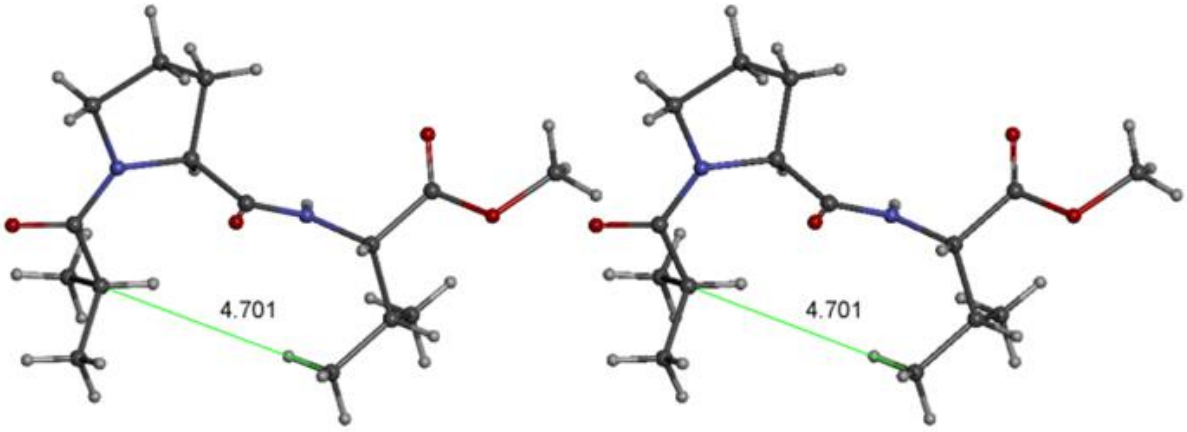

Figure 2. Stereoview of the crystal structure of Ibu-*cis*Pro-Val-OMe (**2**). (Crystallized from EtOAc : Hexane (1:2))

Table 1. A list of selected dihedral angles obtained from the crystal structure of compound **2**.

Conformational Angles (deg)

Peptide Backbone	A	B	Pyrrolidine Ring	A	B
$\omega_1(C^{\alpha}_{Ibu}\text{-}C'_{Ibu}\text{-}N_{Pro}\text{-}C^{\alpha}_{Pro})$	-1.7(7)	-4.9(6)	$\theta(C^{\delta}_{Pro}\text{-}N_{Pro}\text{-}C^{\alpha}_{Pro}\text{-}C^{\beta}_{Pro})$	-11.2(8)	-11.1(1)
$\phi_1(C'_{Ibu}\text{-}N_{Pro}\text{-}C^{\alpha}_{Pro}\text{-}C'_{Pro})$	-77.5(4)	-73.1(6)	$\chi^1_{Pro}(N_{Pro}\text{-}C^{\alpha}_{Pro}\text{-}C^{\beta}_{Pro}\text{-}C^{\gamma}_{Pro})$	31.3(8)	30.4(8)
$\psi_1(N_{Pro}\text{-}C^{\alpha}_{Pro}\text{-}C'_{Pro}\text{-}N_{Val})$	158.4(7)	150.5(8)	$\chi^2_{Pro}(C^{\alpha}_{Pro}\text{-}C^{\beta}_{Pro}\text{-}C^{\gamma}_{Pro}\text{-}C^{\delta}_{Pro})$	-39.7(1)	-38.7(0)
$\omega_2(C^{\alpha}_{Pro}\text{-}C'_{Pro}\text{-}N_{Val}\text{-}C^{\alpha}_{Val})$	169.0(7)	163.8(0)	$\chi^3_{Pro}(C^{\beta}_{Pro}\text{-}C^{\gamma}_{Pro}\text{-}C^{\delta}_{Pro}\text{-}N_{Pro})$	32.5(0)	31.5(7)
$\phi_2(C'_{Pro}\text{-}N_{Val}\text{-}C^{\alpha}_{Val}\text{-}C'_{Val})$	-120.0(4)	-75.0(8)	$\chi^4_{Pro}(C^{\gamma}_{Pro}\text{-}C^{\delta}_{Pro}\text{-}N_{Pro}\text{-}C^{\alpha}_{Pro})$	-13.1(9)	-12.7(2)
$\chi^1_{Val}(N_{Val}\text{-}C^{\alpha}_{Val}\text{-}C^{\beta}_{Val}\text{-}C^{\gamma}_{Val})$	-59.7(5)	-59.8(6)			

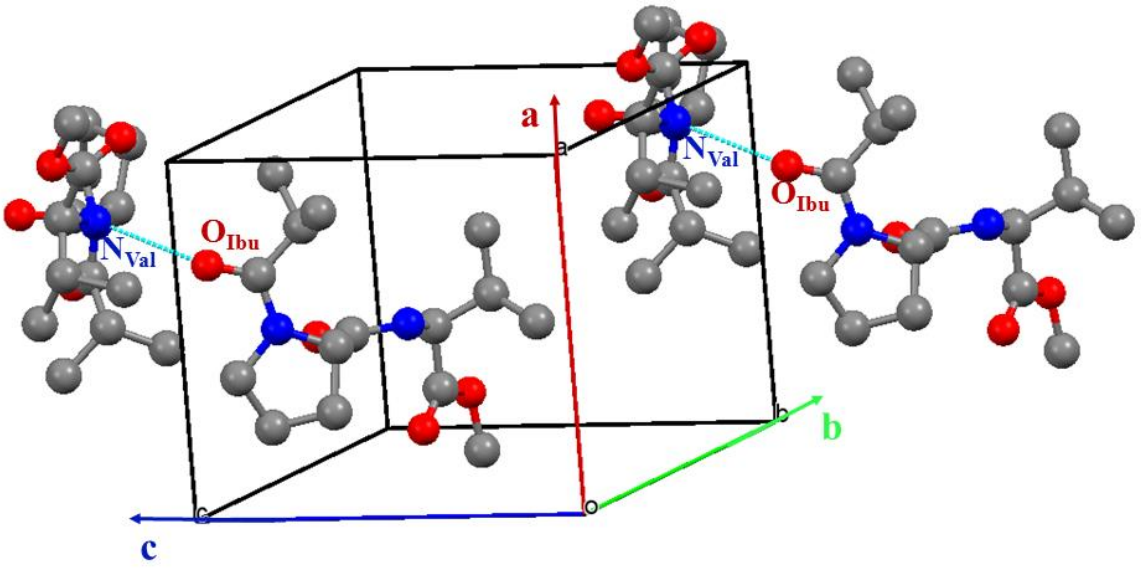

Figure 3. Packing diagram of compound **2** indicating intermolecular hydrogen bonds with the assembly of molecules proceeding along the **c** axis. Hydrogen atoms are not shown for clarity.

Table 2. Crystal and diffraction parameters of **2**.

	2
Empirical formula	$C_{15}H_{26}N_2O_4$
Crystal shape	Block
Crystal size (mm^3)	0.30 x 0.20 x 0.15
Crystal Colour	White
Crystallizing solvent	EtOAc-Hex
Space group	P 1
Space latice	Triclinic
Cell parameters	
a (Å)	8.900(2)
b (Å)	8.958(2)
c (Å)	10.397(2)
α (deg)	92.153(13)
β (deg)	96.035(13)
γ (deg)	94.714(12)
Volume ($Å^3$)	820.6(3)
Z	1
Molecular weight	298.38
Density (g/cm^3) (cal)	1.208
F (000)	324
Radiation (0.71073 Å)	Mo Kα
Temperature (K)	100
2θ max (deg)	52.00
Scan type	ω scan
Measured reflections	12266
Independent reflections	5408
Unique reflections	5408
Observed reflections [|F| > 4σ(F)]	4838
Final R (%)	4.31
Final wR2 (%)	12.18
Goodness-of-fit (S)	0.845
$\Delta \rho_{max}$ ($eÅ^{-3}$)	0.192
$\Delta \rho_{min}$ ($eÅ^{-3}$)	-0.194
No. of restraints / parameters	3/389

S5. Experimental Section

S5.1. Synthesis of Ibu_{i-1}-Pro_i-Xaa_{i+1}-OMe (1-6):

The syntheses of the analogues **1-4, 6** was accomplished using the standard solution phase mixed anhydride peptide coupling protocol in the presence of ethylchloroformate (ECF). The N-terminal of L-Pro (**a**, 0°C, 86.8 mmol) was protected with the acid labile t-butyloxycarbonyl (Boc) group in the presence of ditertiarybutyl dicarbonate $(Boc)_2O$ (91.2 mmol) and two equivalents of potassium carbonate (K_2CO_3, 173.6 mmol) in water (H_2O) : tetrahydrofuran (THF) solvent mixture (1:1) to get N-Boc-Pro-OH (**b**) in excellent yields. N-Boc protected proline was coupled with the desired amino ester hydrochloride salt in the presence of ethyl chloroformate and N-methyl morpholine in THF : DMF solvent mixture to get the corresponding Boc-Pro-Xaa-OMe dipeptides (**c_1-c_4, c_6**) in good yields. Boc deprotection of **c_1-c_4, c_6** in the presence of 20% trifluoroacetic acid in dichloromethane followed by coupling of the resulting secondary ammonium salt with isobutyric acid in the presence of ethyl chloroformate and N-methyl morpholine yielded the desired dipeptide analogues (**1-4, 6**) in good yields.

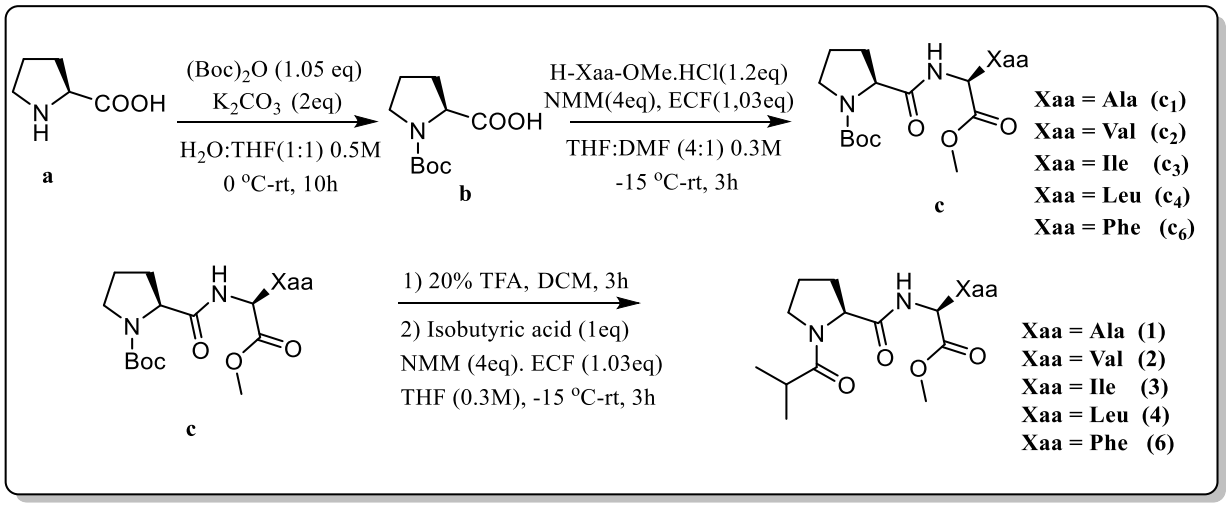

Scheme 1. Synthesis of Ibu_{i-1}-Pro_i-Xaa_{i+1}-OMe (**1-4, 6**).

For the synthesis of **5,** to a cold (0 °C) solution of Ibu-Pro-OH (1.08 mmol), 1-Ethyl-3-(3-dimethylaminopropyl)carbodiimide (EDC.HCl) (1.40 mmol) and HOBt (1.40 mmol) in acetonitrile (MeCN) H-Cha-OMe.HCl (1.19 mmol) was added followed by Diisopropylethylamine (DIPEA) (4.32 mmol) under N_2 atmosphere and vigorously stirred.

After 20 min the mixture was warmed to 25 °C and stirred further until TLC indicated complete consumption of the starting material acid.

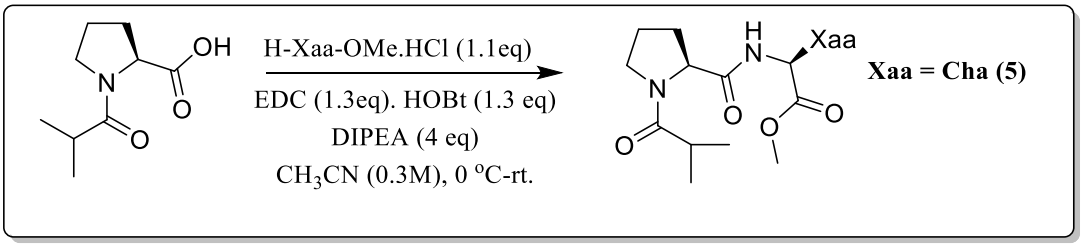

Scheme 2. Synthesis of Ibu_{i-1}-Pro_i-Cha_{i+1}-OMe (**5**).

S6. Purification and Spectral Details

S6.1. ((tert-butoxycarbonyl)-L-proline 2 (b):

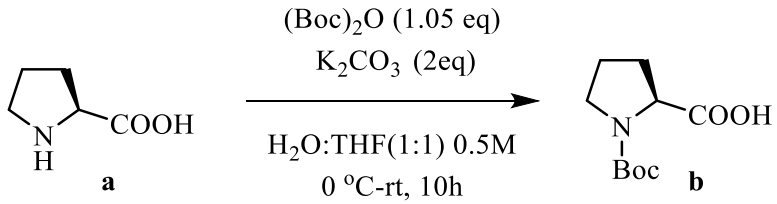

THF was removed and extracted with diethyl ether (2 X 5 mL) to remove the unreacted $(Boc)_2O$. The aqueous layer was acidified to pH = 2, followed by extraction of the product with copious volumes of ethyl acetate to obtain the desired product as white solid (18.1 gm, 84.2 mmol, 97 %), which was used further without any purification.

S6.2. tert-butyl (S)-2-(((S)-1-methoxy-1-oxopropan-2-yl)carbamoyl)pyrrolidine-1-carboxylate c_1 :

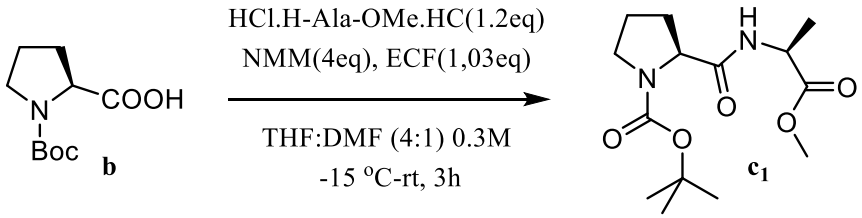

Removal of solvent resulted in a residue which was dissolved in ethyl acetate (EtOAc) (20 mL), washed with 10 mL water (2 X 5 mL) and 1N HCl solution (2 X 5 mL) and saturated $NaHCO_3$ solution (2 X 5 mL). The organic layer was dried over anhydrous sodium sulphate (Na_2SO_4) and

concentrated to get a residue which was purified by silica gel (100-200 mesh) flash column chromatography (EtOAc : Hexane – 1 : 8) yielded the desired product as a white solid (1291 mg, 4.30 mmol, 93% yield); (mp 71-73 ^{o}C); (TLC- EtOAc – R_f = 0.56); IR (NaCl, 10 mM in $CHCl_3$): 3419, 3323, 2984, 1743, 1682, 1516, 1455, 1394, 1256 cm^{-1}; HRMS *m/z* Calcd for $C_{14}H_{24}N_2O_5Na$ 323.1583 (M+Na), Found 323.1583.

S6.3. tert-butyl (S)-2-(((S)-1-methoxy-3-methyl-1-oxobutan-2-yl)carbamoyl)pyrrolidine-1-carboxylate (c_2):

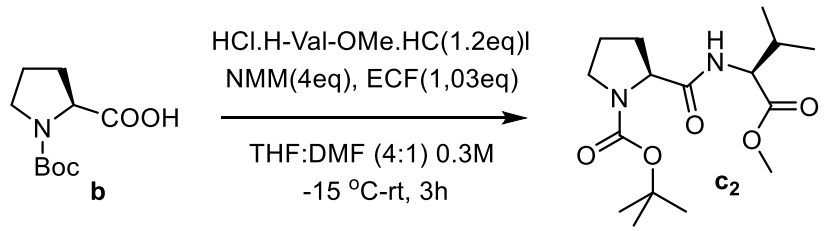

Removal of solvent resulted in a residue which was dissolved in ethyl acetate (EtOAc) (20 mL), washed with 10 mL water (2 X 5 mL) and 1N HCl solution (2 X 5 mL) and saturated $NaHCO_3$ solution (2 X 5 mL). The organic layer was dried over anhydrous sodium sulphate (Na_2SO_4) and concentrated to get a residue which was purified by silica gel (100-200 mesh) flash column chromatography (EtOAc : Hexane – 1 : 15) yielded the desired product as a white solid (1388 mg, 4.23 mmol, 91% yield); (mp 64-66 ^{o}C); (TLC- EtOAc – R_f = 0.63); IR (NaCl, 10 mM in $CHCl_3$): 3417, 3318 , 2972, 1741, 1682, 1603, 1517, 1438, 1394, 1265 cm^{-1}; HRMS *m/z* Calcd for $C_{16}H_{28}N_2O_5Na$ 351.1896 (M+Na), Found 351.1892.

S6.4. tert-butyl (S)-2-(((2S,3R)-1-methoxy-3-methyl-1-oxopentan-2-yl) carbamoyl) pyrrolidine-1-carboxylate (c_3):

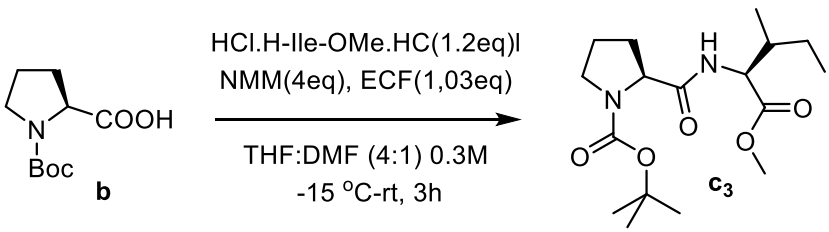

Removal of solvent resulted in a residue which was dissolved in ethyl acetate (EtOAc) (15 mL), washed with 10 mL water (2 X 5 mL) and 1N HCl solution (2 X 5 mL) and saturated $NaHCO_3$ solution (2 X 5 mL). The organic layer was dried over anhydrous sodium sulphate (Na_2SO_4) and

concentrated to get a residue which was purified by silica gel (100-200 mesh) flash column chromatography (EtOAc : Hexane – 1 : 9) yielded the desired product as a viscous liquid (683 mg, 2.00 mmol, 86% yield); (TLC- EtOAc – R_f = 0.63); IR (NaCl, 10 mM in $CHCl_3$): 3422, 3315, 2960, 1743, 1682, 1602, 1518, 1438, 1394, 1262 cm^{-1}; HRMS *m/z* Calcd for $C_{17}H_{30}N_2O_5Na$ 365.2052 (M+Na), Found 365.2054.

S6.5. tert-butyl (S)-2-(((S)-1-methoxy-4-methyl-1-oxopentan-2-yl)carbamoyl)pyrrolidine-1-carboxylate (c_4):

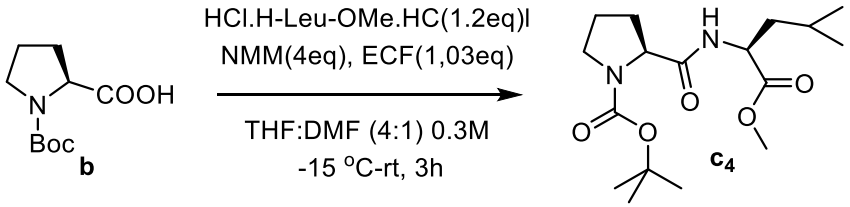

Removal of solvent resulted in a residue which was dissolved in ethyl acetate (EtOAc) (15 mL), washed with 10 mL water (2 X 5 mL) and 1N HCl solution (2 X 5 mL) and saturated $NaHCO_3$ solution (2 X 5 mL). The organic layer was dried over anhydrous sodium sulphate (Na_2SO_4) and concentrated to get a residue which was purified by silica gel (100-200 mesh) flash column chromatography (EtOAc : Hexane – 1 : 9) yielded the desired product as a white solid (883 mg, 2.58 mmol, 92% yield); (mp 89-91 °C); (TLC- EtOAc – R_f = 0.63); IR (NaCl, 10 mM in $CHCl_3$): 3422, 3313, 2960, 1743, 1682, 1624, 1518, 1438, 1395, 1291 cm^{-1}; HRMS *m/z* Calcd for $C_{17}H_{30}N_2O_5Na$ 365.2052 (M+Na), Found 365.2052.

S6.6. tert-butyl (S)-2-(((S)-1-methoxy-1-oxo-3-phenylpropan-2-yl)carbamoyl)pyrrolidine-1-carboxylate (c_6) :

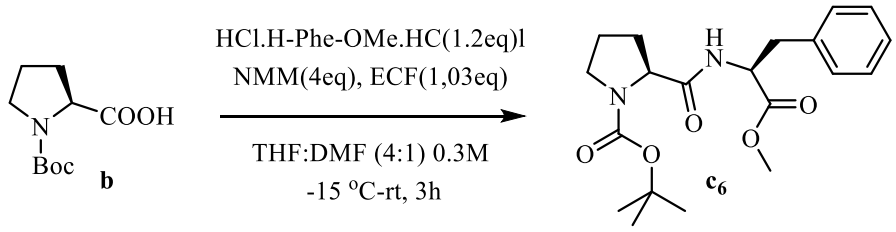

Removal of solvent resulted in a residue which was dissolved in ethyl acetate (EtOAc) (20 mL), washed with 10 mL water (2 X 5 mL) and 1N HCl solution (2 X 5 mL) and saturated $NaHCO_3$ solution (2 X 5 mL). The organic layer was dried over anhydrous sodium sulphate (Na_2SO_4) and concentrated to get a residue which was purified by silica gel (100-200 mesh) flash column chromatography (EtOAc : Hexane – 1 : 9) yielded the desired product as a white solid (1594 mg, 4.24 mmol, 91% yield); (mp 72 – 74 °C); (TLC- EtOAc – R_f = 0.63); **FTIR** (NaCl, 10 mM in

$CHCl_3$): 3420, 3311, 2983, 1745, 1681, 1516, 1438, 1394, 1258 cm^{-1}. HRMS *m/z* Calcd for $C_{20}H_{28}N_2O_5Na$ 399.1896 (M+Na), Found 399.1893.

S6.7. Methyl-N-isobutyroyl-L-prolyl-L-alaninate (1)

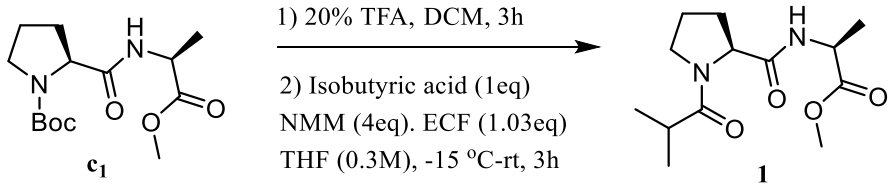

After Boc-deprotection, solvent was removed under vacuum connected to KOH trap to obtain the desired TFA salt product as viscous oil (314 mg, 1.00 mmol, 100% yield), which was directly used for further reactions.

Removal of solvent after coupling reaction resulted in a residue which was dissolved in ethyl acetate (EtOAc) (15 mL), washed with 10 mL water (2 X 5 mL) and 1N HCl solution (2 X 5 mL) and saturated $NaHCO_3$ solution (2 X 5 mL). The organic layer was dried over anhydrous sodium sulphate (Na_2SO_4) and concentrated to get a residue which was purified by silica gel (100-200 mesh) flash column chromatography (EtOAc : Hexane – 3 : 7) yielded the desired product as a viscous liquid (211 mg, 0.78 mmol, 78% yield); (TLC- EtOAc) – R_f = 0.34); IR (NaCl, 10 mM in $CHCl_3$): 3447, 3422, 3291, 2983, 1743, 1677, 1624, 1522, 1436, 1321, 1241 cm^{-1}; HRMS *m/z* Calcd for $C_{13}H_{22}N_2O_4Na$ 293.1477 (M+Na), Found 293.1478.

S6.8. Methyl-N-isobutyroyl-L-prolyl-L-valinate (2):

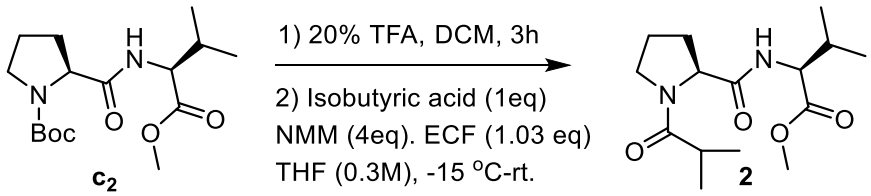

After Boc-deprotection, solvent was removed under vacuum connected to KOH trap to obtain the desired TFA salt product as viscous oil (313 mg, 0.91 mmol, 100% yield), which was directly used for further reactions.

Removal of solvent after coupling reaction resulted in a residue which was dissolved in ethyl acetate (EtOAc) (15 mL), washed with 10 mL water (2 X 5 mL) and 1N HCl solution (2 X 5 mL) and saturated $NaHCO_3$ solution (2 X 5 mL). The organic layer was dried over anhydrous sodium

sulphate (Na_2SO_4) and concentrated to get a residue which was purified by silica gel (100-200 mesh) flash column chromatography (EtOAc : Hexane – 1 : 4) yielded the desired product as a white solid (207 mg, 0.69 mmol, 76% yield); (mp 91-93 ^oC); (TLC- EtOAc) – R_f = 0.50); IR (NaCl, 10 mM in $CHCl_3$): 3426, 3297, 2971, 1742, 1678, 1620, 1537, 1431, 1322, 1210 cm^{-1}; HRMS *m/z* Calcd for $C_{15}H_{26}N_2O_4Na$ 321.1790 (M+Na), Found 321.1793.

S6.9. Methyl-N-isobutyroyl-L-prolyl-L-alloisoleucinate (3):

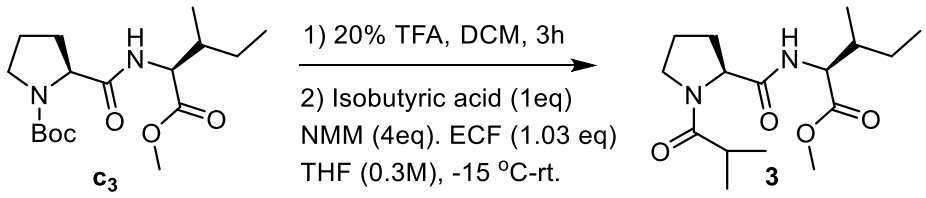

After Boc-deprotection, solvent was removed under vacuum connected to KOH trap to obtain the desired TFA salt product as viscous oil (312 mg, 0.88 mmol, 100% yield), which was directly used for further reactions.

Removal of solvent after coupling reaction resulted in a residue which was dissolved in ethyl acetate (EtOAc) (15 mL), washed with 10 mL water (2 X 5 mL) and 1N HCl solution (2 X 5 mL) and saturated $NaHCO_3$ solution (2 X 5 mL). The organic layer was dried over anhydrous sodium sulphate (Na_2SO_4) and concentrated to get a residue which was purified by silica gel (100-200 mesh) flash column chromatography (EtOAc : Hexane – 1 : 4) yielded the desired product as a viscous liquid (212 mg, 0.68 mmol, 77% yield); (TLC- EtOAc) – R_f = 0.50); IR (NaCl, 10 mM in $CHCl_3$): 3423, 3298, 2962, 1743, 1678, 1621, 1532, 1431, 1322, 1259 cm^{-1}; HRMS *m/z* Calcd for $C_{16}H_{28}N_2O_4Na$ 335.1947 (M+Na), Found 335.1947.

S6.10. Methyl-N-isobutyroyl-L-prolyl-L-leucinate (4):

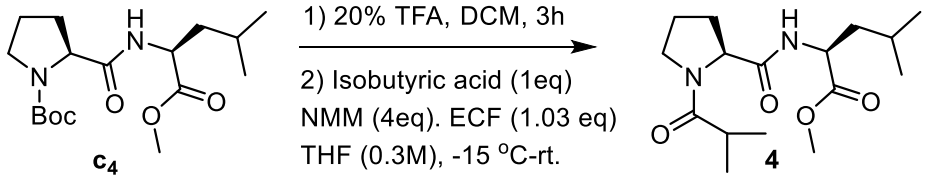

After Boc-deprotection, solvent was removed under vacuum connected to KOH trap to obtain the desired TFA salt product as viscous oil (312 mg, 0.88 mmol, 100% yield), which was directly used for further reactions.

Removal of solvent after the coupling reaction resulted in a residue which was dissolved in ethyl acetate (EtOAc) (15 mL), washed with 10 mL water (2 X 5 mL) and 1N HCl solution (2 X 5 mL) and saturated $NaHCO_3$ solution (2 X 5 mL). The organic layer was dried over anhydrous sodium sulphate (Na_2SO_4) and concentrated to get a residue which was purified by silica gel (100-200 mesh) flash column chromatography (EtOAc : Hexane – 1 : 4) yielded the desired product as a viscous liquid (215 mg, 0.69 mmol, 78% yield); (TLC- EtOAc) – R_f = 0.50); IR (NaCl, 10 mM in $CHCl_3$): 3422, 3293, 2962, 1743, 1679, 1619, 1540, 1436, 1321, 1279 cm^{-1}; HRMS *m/z* Calcd for $C_{16}H_{28}N_2O_4Na$ 335.1947 (M+Na), Found 335.1943.

S6.11. Methyl-N-isobutyroyl-prolyl-phenylalaninyl-ester (6):

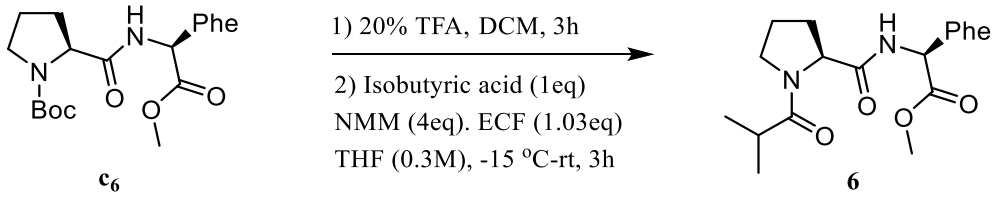

c_6 **6**

After Boc-deprotection, solvent was removed under vacuum connected to KOH trap to obtain the desired TFA salt product as viscous oil (311 mg, 0.80 mmol, 100% yield), which was directly used for further reactions.

Removal of solvent after the coupling reaction resulted in a residue which was dissolved in ethyl acetate (EtOAc) (15 mL), washed with 10 mL water (2 X 5 mL) and 1N HCl solution (2 X 5 mL) and saturated $NaHCO_3$ solution (2 X 5 mL). The organic layer was dried over anhydrous sodium sulphate (Na_2SO_4) and concentrated to get a residue which was purified by silica gel (100-200 mesh) flash column chromatography (EtOAc : Hexane – 1 : 4) which yielded the desired product as a white solid (218 mg, 0.63 mmol, 79% yield); (mp 53-55 °C); (TLC- EtOAc) – R_f = 0.5); IR (NaCl, 10 mM in $CHCl_3$): 3422, 3287, 2960, 1745, 1676, 1623, 1520, 1438, 1217 cm^{-1}; HRMS *m/z* Calcd for $C_{19}H_{26}N_2O_4Na$ 369.1790 (M+Na), Found 369.1785.

S6.12. methyl (S)-3-cyclohexyl-2-((S)-1-isobutyroylpyrrolidine-2-carboxamido)propanoate (5):

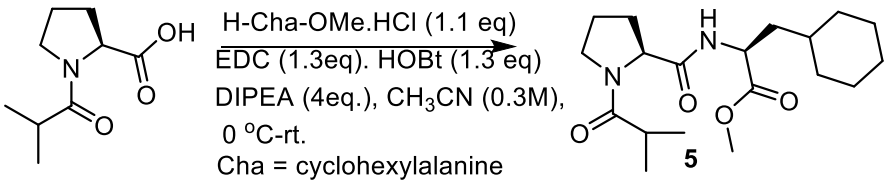

Removal of solvent resulted in a residue which was dissolved in ethyl acetate (EtOAc) (15 mL), washed with 10 mL water (2 X 5 mL) and 1N HCl solution (2 X 5 mL) and saturated $NaHCO_3$ solution (2 X 5 mL). The organic layer was dried over anhydrous sodium sulphate (Na_2SO_4) and concentrated to get a residue which was purified by silica gel (100-200 mesh) flash column chromatography (EtOAc : Hexane – 1 : 4) yielded the desired product as a viscous liquid (27 mg, 0.08 mmol, 79% yield); (TLC- EtOAc) – R_f = 0.50); IR (NaCl, 10 mM in $CHCl_3$): 3427, 3294, 2928, 1743, 1676, 1621, 1526, 1436, 1322, 1217 cm^{-1}. HRMS *m/z* Calcd for $C_{19}H_{32}N_2O_4Na$ 375.2260 (M+Na), Found 375.2259.

S7. Conformational analyses from 2D-NMR spectra

The ^{1}H NMR signals sets corresponding to the cis/trans rotamers were assigned based on analyses of their 2D TOCSY, HSQC and ROESY spectra (20 mM, 300K). Homonuclear H,H 2D TOCSY spectra revealed the ^{1}H signals corresponding to each of the individual spin systems in every single rotamer as they exhibit $^{n}J_{H,H}$ scalar coupling with each other through bonds.

S7.1. 2D NMR spectra of Ibu$_{-1}$-Pro$_{i}$-Xaa$_{i+1}$-OMe (1-6) analogues

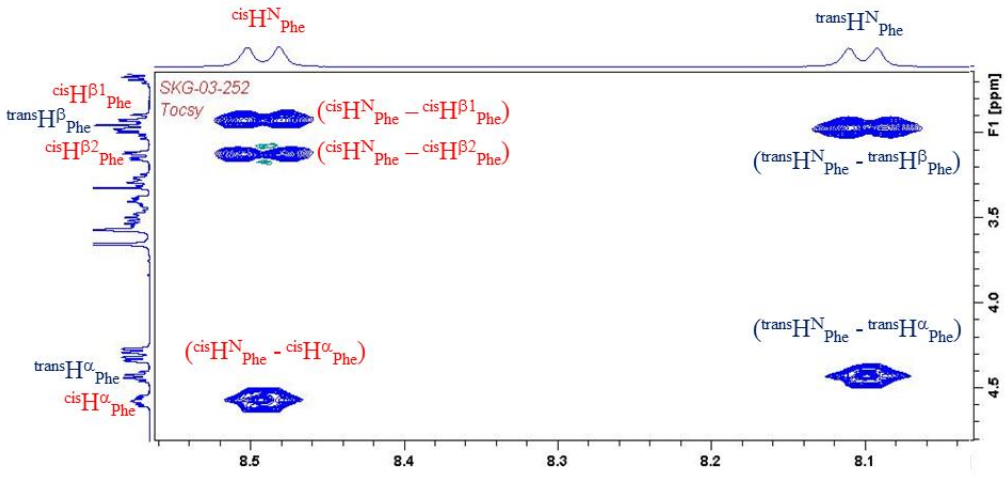

Figure 4. Relevant portions of the 2D TOCSY spectrum of iBu$_{i-1}$-Pro$_{i}$-Phe$_{i+1}$-OMe (**6**) in DMSO-d$_6$, 20 mM, 300 K.

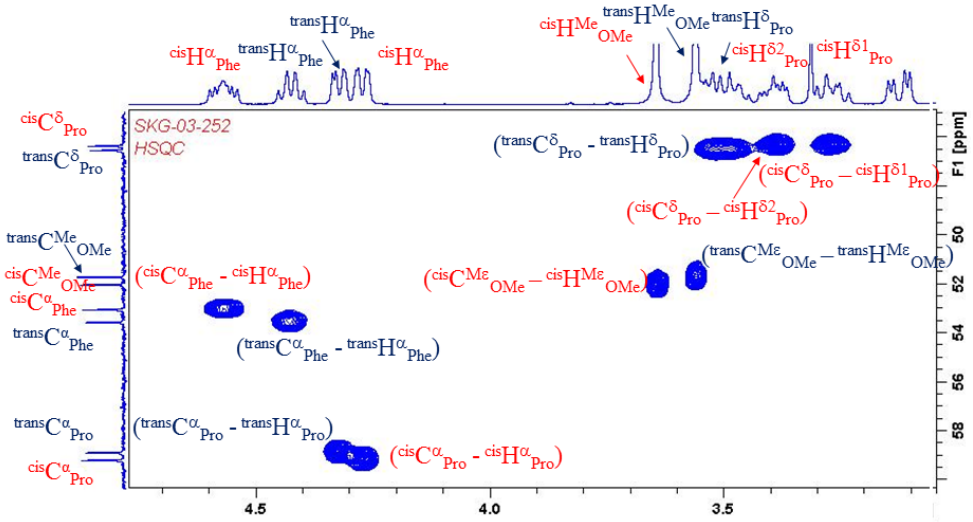

Figure 5. Relevant portions of the 2D HSQC spectrum of iBu$_{i-1}$-Pro$_{i}$-Phe$_{i+1}$-OMe (**6**) in DMSO-d$_6$, 20 mM, 300 K.

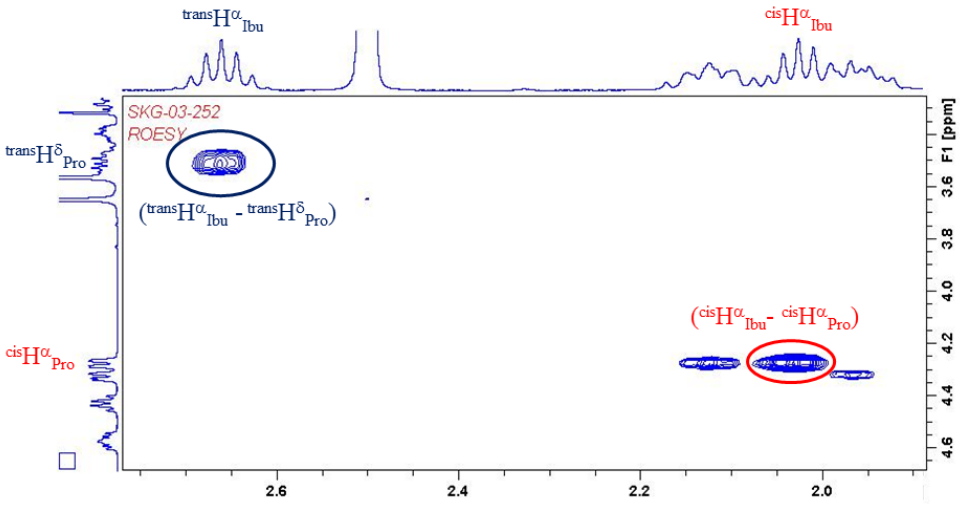

Figure 6. Relevant portions of the 2D ROESY spectrum of Ibu$_{i-1}$-Pro$_i$-Phe$_{i+1}$-OMe (**6**) in DMSO-d6, 20 mM, 300 K, highlighting the cross peaks characteristic for *cis*Pro and *trans*Pro rotamers.

The ROESY spectrum showed a C$^{\alpha}_{Ibu(i-1)}$-H$^{\alpha}$···H$^{\delta}$-Phe$_{i+1}$ (i-1…i+1) cross peak exclusively in the *cis*Pro conformer. No such cross peaks were observed in the *trans*Pro isomer of **6**.

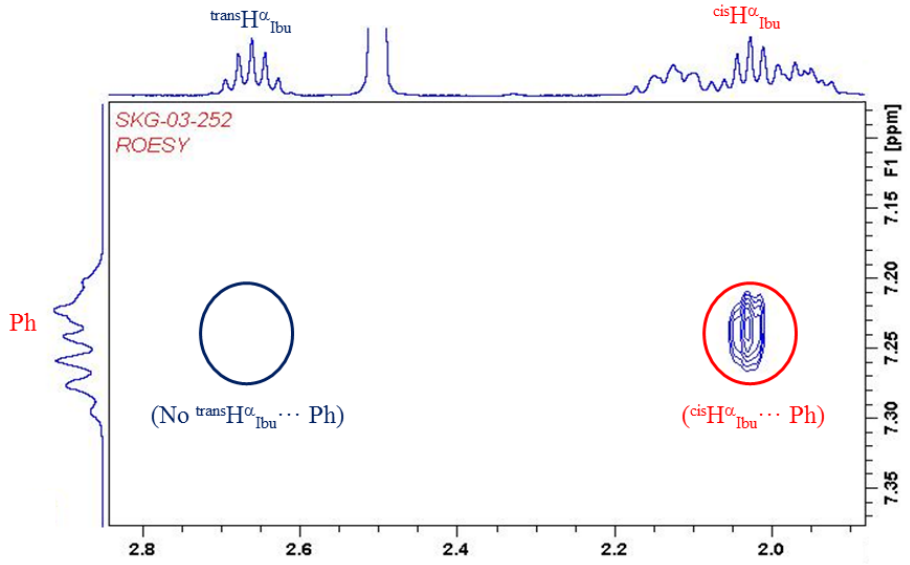

Figure 7. Relevant portions of the 2D ROESY spectrum of Ibu$_{i-1}$-Pro$_i$-Phe$_{i+1}$-OMe (**6**) in DMSO-d6, 20 mM, 300 K, highlighting the cross peaks characterizing the C$^{\alpha}_{Ibu(i-1)}$-H···Phe$_{i+1}$ interaction in the *cis*Pro rotamer.

Note that these H$^{\alpha}_{Ibu(i-1)}$···S.C.$_{i+1}$ cross peaks (DMSO-d$_6$) are either too weak to observe or are absent in the Ala analogue **1**.

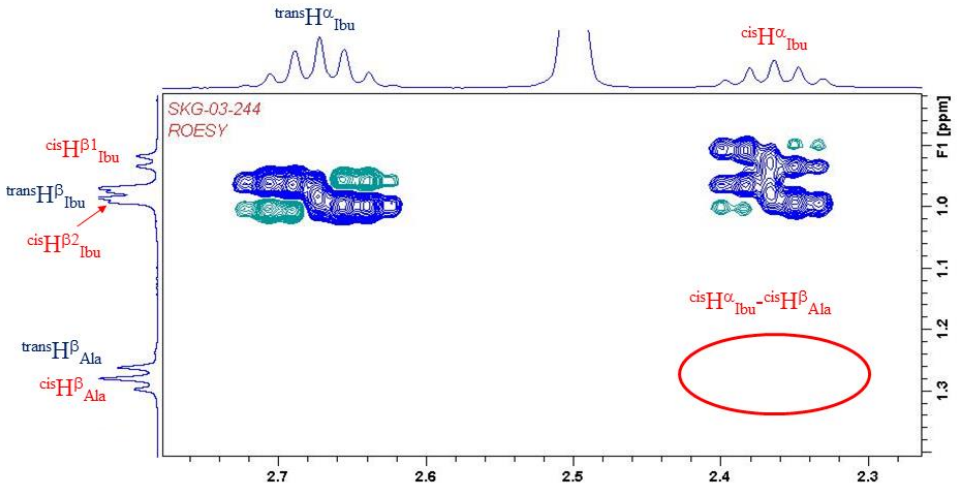

Figure 8: Partial 2D ROESY spectrum of Ibu_{i-1}-Pro_i-Ala_{i+1}-OMe (**1**), showing no cross peaks between the Ala side chain and the H^{α}_{Ibu} signals.

Remarkably the 2D ROESY spectrum of Leu analogue (**4**) (DMSO-d_6), containing the longer aliphatic side chain, reveals the presence of the crucial $H^{\alpha}_{Ibu(i-1)}\cdots H^{\delta 2}_{Leu(i+1)}$ NOE weak cross peak.

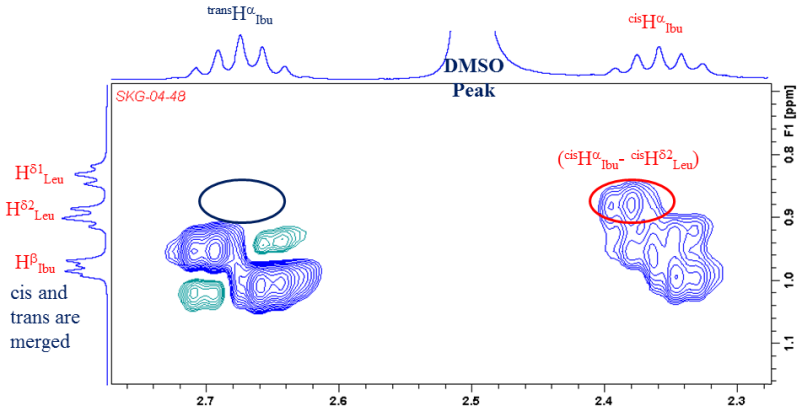

Figure 9: Partial 2D ROESY spectrum of Ibu_{i-1}-Pro_i-Leu_{i+1}-OMe (**4**) highlighting the $H^{\alpha}_{Ibu(i-1)}\cdots H^{\delta 2}_{Leu(i+1)}$ cross peak, signifying the proximity between isopropyl groups of the Ibu group and the Leu residue.

The aliphatic region of 2D ROESY spectrum of Cha analogue (**5**) is complicated due to presence of a number of overlapping groups and hence cannot be interpreted without sufficient ambiguity.

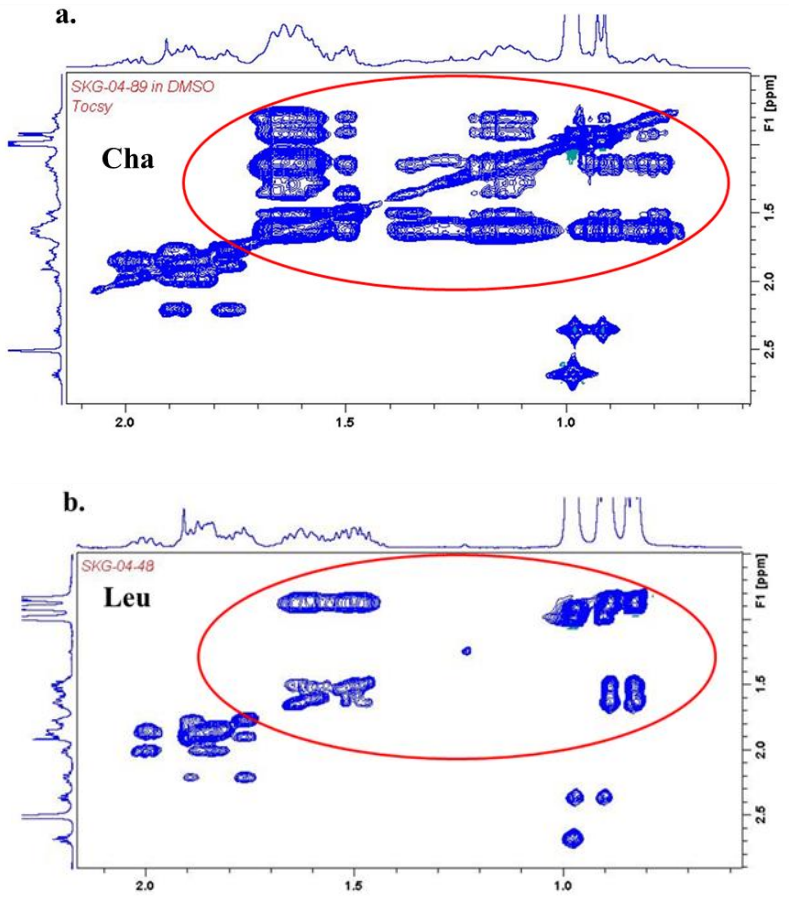

Figure 10a,b. Partial 2D TOCSY spectra of Ibu_{i-1}-Pro_i-Cha_{i+1}-OMe (**5**) and Ibu_{i-1}-Pro_i-Leu_{i+1}-OMe (**4**) in DMSO-d_6 (Cha is cyclohexylalanine).

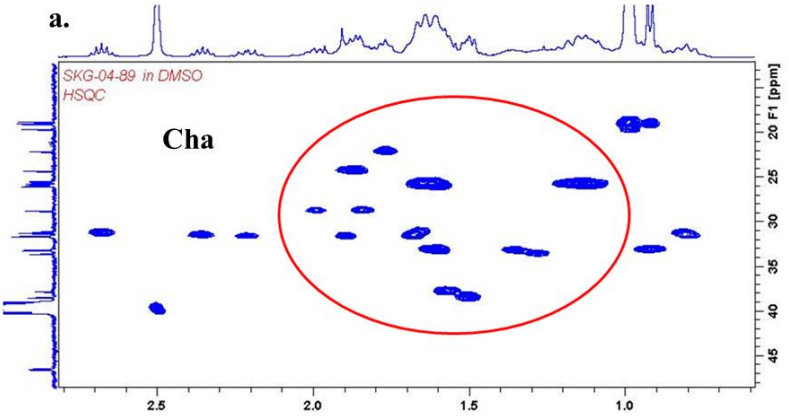

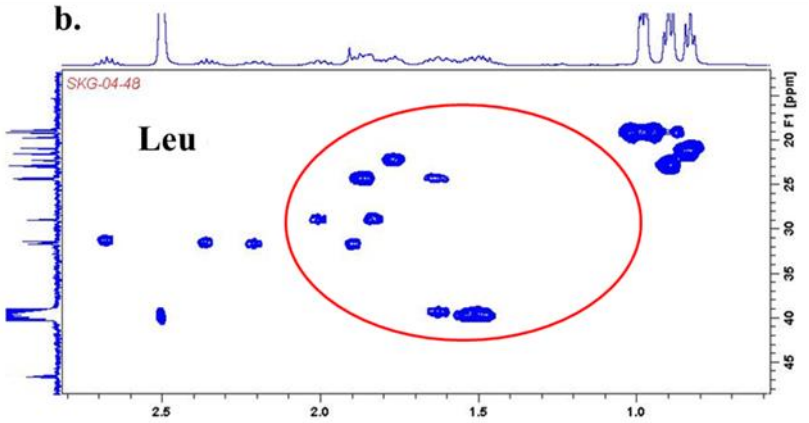

Figure 11a,b. Partial 2D HSQC spectra of Ibu_{i-1}-Pro_i-Cha_{i+1}-OMe (**5**) and Ibu_{i-1}-Pro_i-Leu_{i+1}-OMe (**4**) in DMSO-d_6.

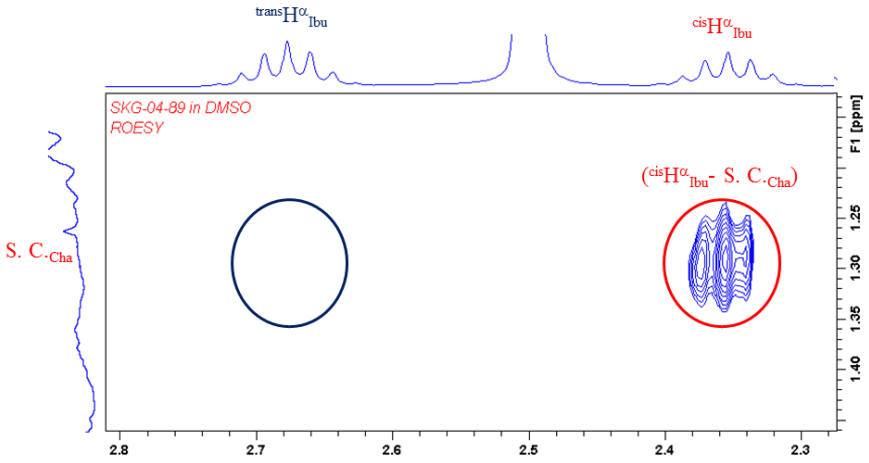

Figure 12. Relevant ROESY spectrum of Ibu_{i-1}-Pro_i-Cha_{i+1}-OMe (**5**), DMSO-d_6, 10mM.

S8. ^{1}H and ^{13}C NMR Tables

S8.1. Assignment of ^{1}H NMR peaks in DMSO-d6

Table 3. ^{1}H NMR of Ibu-Pro-Alp-OMe (1-5) in DMSO-d_6 (400 MHz, 10 mM)

	Ibu-Pro-Ala-OMe (1) (DMSO-d_6)		**Ibu-Pro-Val-OMe (2) (DMSO-d_6)**	
	cis **δ (ppm)**	***trans*** **δ (ppm)**	***cis*** **δ (ppm)**	***trans*** **δ (ppm)**
Ibu–H$^{\alpha}$	2.36 (sept, J = 6.8 Hz)	2.67 (sept, J = 6.8 Hz)	2.39 (sept, J = 6.4 Hz)	2.68 (sept, J = 6.8 Hz)
H$^{\beta}$	0.98 (d, J = 6.4 Hz)	0.98 (d, J = 6.4 Hz)	0.86 (d, J = 6.8 Hz)	0.99 (d, J = 6.4 Hz)
	0.92 (d, J = 6.4 Hz)	0.97 (d, J = 6.4 Hz)		-
Pro-H$^{\alpha}$	4.39 (dd, J = 8.4, 2.4 Hz)	4.30 (dd, J = 8.8, 3.6 Hz)	4.54 (d, J = 7.2 Hz)	4.42 (dd, J = 9.2, 2.4 Hz)
H$^{\beta}$	2.19 (qu, J = 8.8 Hz)	2.07-1.98 (m)	2.27-2.15 (m)	2.25-1.94 (m)
	1.97 -1.90 (m)	1.88-1.79 (m)		1.87-1.82 (m)
H$^{\gamma}$	1.80-1.71 (m)	1.95-1.80 (m)	1.81-1.71 (m)	1.91-1.83 (m)
H$^{\delta}$	3.48-3.40 (m)	3.59-3.48 (m)	3.48-3.38 (m)	3.59-3.48 (m)
	3.33 (t, J = 8.0 Hz)		3.37-3.27 (m)	
Aro N-H	8.49 (d, J = 7.2 Hz)	8.20 (d, J = 7.2 Hz)	8.39 (d, J = 8.4 Hz)	8.05 (d, J = 7.6 Hz)
H$^{\alpha}$	4.30 (qu, J = 7.2 Hz)	4.22 (qu, J = 7.2 Hz)	4.23 (dd, J = 8.0, 6.4 Hz)	4.12 (dd, J = 7.6, 6.4 Hz)
H$^{\beta}$	1.28 (d, J = 7.2 Hz)	1.27 (d, J = 7.2 Hz)	2.14-2.07 (m)	2.06-1.94 (m)
H$^{\beta}$			0.86 (d, J = 6.8 Hz)	0.88 (d, J = 6.4 Hz)
OCH_3	3.62 (s)	3.61 (s)	3.64 (s)	3.62 (s)

^{1}H NMR of Ibu-Pro-Alp-OMe in DMSO-d_6 (400 MHz, 10 mM, 300 K)

	Ibu-Pro-Ile-OMe (3) (DMSO-d_6)		**Ibu-Pro-Leu-OMe (4) (DMSO-d_6)**		**Ibu-Pro-Cha-OMe (5) (DMSO-d_6)**	
	cis **δ (ppm)**	***trans*** **δ (ppm)**	***cis*** **δ (ppm)**	***trans*** **δ (ppm)**	***cis*** **δ (ppm)**	***trans*** **δ (ppm)**
Ibu–H^{α}	2.38 (sept, J = 6.8 Hz)	2.36 (sept, 6.4 Hz)	2.67 (sept, 6.8 Hz)	2.69 (sept, J = 6.8 Hz)	2.35 (sept, J = 6.8 Hz)	2.68 (sept, J = 6.8 Hz)
H^{β}	0.98 (d, J = 6.8 Hz)	0.97 (d, J = 6.8 Hz)	0.98 (d, J = 6.4 Hz)	0.99 (d, J = 6.8 Hz)	0.98 (d, J = 6.4 Hz)	0.99 (d, J = 6.4 Hz)
	0.88 (d, J = 6.8 Hz)	0.90 (d, J = 6.8 Hz)	0.97 (d, J = 6.4 Hz)	0.98 (d, J = 6.8 Hz)	0.92 (d, J = 6.4 Hz)	
Pro-H^{α}	4.53 (dd, J = 8.8, 2.4 Hz)	4.41 (dd, 8.4, 1.6 Hz)	4.32 (dd, J = 9.2, 2.8 Hz)	4.42 (dd, J = 7.2, 2.8 Hz)	4.42 (dd, J = 8.8, 2.4 Hz)	4.33 (dd, J = 8.4, 2.4 Hz)
H^{β}	1.91 – 1.85(m)	2.21 (qu, J = 8.8 Hz)	2.00 (qu, J = 8.0 Hz)	1.90 – 1.82 (m)	1.93-1.87(m)	1.89-1.80(m)
	2.24 – 2.18 (m)	1.93-1.87 (m)	1.87-1.80 (m)	2.01 – 1.93 (m)	2.25-2.17(m)	2.04-1.94(m)
H^{γ}	1.81 – 1.73 (m)	1.82-1.73 (m)	1.92-1.82 (m)	1.92 – 1.82 (m)	1.82-1.72 (m)	1.94-1.82 (m)
H^{δ}	3.46 – 3.41 (m)	3.48-3.44 (m)	3.57-3.48 – (m)	3.58 – 3.48 (m)	3.49-3.43(m)	3.54-3.48(m)
	3.36 – 3.30 (m)	3.36-3.28 (m)	3.53-4.48 (m)		3.36-3.30(m)	3.58-3.52(m)
Aro N-H	8.39 (d, J = 8.4 Hz)	8.47 (d, J = 8.0 Hz)	8.11 (d, 7.2 Hz)	8.03 (d, J = 8.4 Hz)	8.47 (d, J = 8.4 Hz)	8.09 (d, J = 7.2 Hz)
H^{α}	4.26 (dd, J = 8.0 Hz, 6.8 Hz)	4.38-4.33 (m)	4.23-4.17 (m)	4.17 (dd, J = 8.0 Hz, 6.4 Hz)	4.37 (dd, J = 8.4, 5.2 Hz)	4.26 (dd, J = 14.8, 7.6 Hz)
H^{β}	1.88 – 1.80 (m)	1.66-1.59 (m)	1.58-1.44 (m)	1.80 – 1.72 (m)	1.60-1.54 (m)	1.53-1.49 (m)
H^{γ}	1.24 – 1.14 (m)	1.55-1.44 (m)	1.55-1.44 (m)	1.24 – 1.14 (m)		
H^{γ}	1.44 – 1.34 (m)			1.44 – 1.34 (m)		
$H^{\gamma'}$	0.86 – 0.82 (m)			0.86 – 0.82 (m)		
H^{δ}	0.86 – 0.82 (m)	0.90-0.89 (merged)	0.89 (d, J = 6.0 Hz)	0.86 – 0.82 (m)		
$H^{\delta'}$		0.82 (d, J = 6.0 Hz)	0.84 (d, J = 6.0 Hz)			
OCH_3	3.64 (s, 3H)	3.62 (s)	3.60 (s)	3.62 (s, 3H)	3.62 (s)	3.60 (s)
Others					1.71-1.59 (m) 1.22-1.06 (m) (4H) 1.03-0.87 (m) 4 H) 0.83-0.75 (m) (2 H)	1.71-1.59 (m) 1.22-1.06 (m) (4 H) 1.03-0.87 (m) 4 H) 0.83-0.75 (m) (2 H)

Table 4. ^{1}H NMR of Ibu-Pro-Phe-OMe (6) in DMSO-d_6 (400 MHz, 10 mM)

	Ibu-Pro-Phe-OMe (6) (DMSO-d_6)	
	cis **δ (ppm)**	***trans*** **δ (ppm)**
Ibu – H^{α}	2.03 (sept, J = 7.2 Hz)	2.64 (sept, 6.8 Hz)
H^{β}	0.88 (d, J = 6.8 Hz)	0.97 (d, J = 6.8 Hz)
	0.70 (d, J = 6.4 Hz)	
Pro – H^{α}	4.27 (dd, J = 8.4, 2.0 Hz)	4.32 (dd, J = 9.2, 2.8 Hz)
H^{β}	2.12 (qu, J = 6.8 Hz)	2.00-1.93 (m)
	1.80-1.72 (m)	1.85-1.80 (m)
H^{γ}	1.73-1.57 (m)	1.80-1.78 (m)
H^{δ}	3.39 (ddd, J = 19.2, 7.6, 3.6 Hz)	3.56-3.44 (m)
	3.32-3.26 (m)	
Aro N-H	8.49 (d, J = 7.2 Hz)	8.10 (d, J = 7.6 Hz)
Ha	4.57 (ddd, J = 19.2, 10.8, 4.4 Hz)	4.42 (q, J = 7.2 Hz)
H^{β}	3.12 (dd, J = 13.6, 4.4 Hz)	2.90 (dt, J = 13.6, 6.0 Hz)
H^{β}	2.91 (dd, J = 13.2, 10.8 Hz)	2.95 (d, J = 8.0 Hz)
HAro	7.29-7.20 (m)	7.29-7.20 (m)
OCH_3	3.64 (s)	3.56 (s)

S8.2. Assignment of ^{13}C NMR peaks in DMSO-d6

Table 5. ^{13}C NMR of Ibu-Pro-Alp-OMe (1-5) in DMSO-d_6 (100 MHz, 60 mM)

	Ibu-Pro-Ala-OMe (1) (DMSO-d_6)		**Ibu-Pro-Val-OMe (2) (DMSO-d_6)**	
	cis **δ (ppm)**	***trans*** **δ (ppm)**	***cis*** **δ (ppm)**	***trans*** **δ (ppm)**
Ibu – C^{α}	31.5	31.2	31.4	31.3
Ibu – C^{β}	19.6, 19.1	19.0, 18.8	19.0, 19.6	18.7, 19.1
Ibu - C′	175.0	174.4	174.8	174.7
Pro – C^{α}	59.2	58.6	58.9	58.6
C^{β}	31.6	29.0	31.7	28.5
C^{γ}	22.1	24.2	22.2	24.3
C^{δ}	46.4	46.6	46.4	46.6
C′	172.1	171.9	172.6	171.96
Alp – C^{α}	47.5	47.4	57.2	57.3
C^{β}	16.83	16.85	29.7	29.96
C^{γ}	-	-	18.0, 18.94	18.1, 18.9
C^{δ}	-	-		
OMe –C′	172.7	173.1	171.8	171.96
OMe –CH_3	51.9	51.8	51.8	51.6
Others	-	-		

	Ibu-Pro-Ile-OMe (3) (DMSO-d_6)		**Ibu-Pro-Leu-OMe (4) (DMSO-d_6)**		**Ibu-Pro-Cha-OMe (5) (DMSO-d_6)**	
	cis **δ (ppm)**	***trans*** **δ (ppm)**	***cis*** **δ (ppm)**	***trans*** **δ (ppm)**	***cis*** **δ (ppm)**	***trans*** **δ (ppm)**
Ibu – C^{α}	31.4	31.6	31.3	31.3	31.5	31.2
Ibu – C^{β}	19.6	19.6	19.0	19.04	19.0	18.7
Ibu – C^{β}	19.0	19.01	18.8	18.7	19.5	18.9
Ibu - C′	174.8	174.9	174.5	174.7	174.8	174.5
Pro – C^{α}	58.9	59.2	58.7	58.6	59.1	58.7
C^{β}	31.6	31.6	28.9	28.5	31.6	28.7
C^{γ}	22.1	22.2	24.2	24.3	22.0	24.2
C^{δ}	46.4	46.5	46.6	46.6	46.4	46.5
C′	171.8	172.4	172.0	171.9	172.3	172.0
Alp – C^{α}	56.2	50.0	50.3	56.3	49.2	49.5
C^{β}	36.0	39.3	39.6	36.4	37.7	38.4
C^{γ}	24.6	24.31	24.28	24.7		
$C^{\gamma'}$	15.41			15.39		
C^{δ}	10.9	22.9	22.7	11.2		
C^{δ}		20.8	21.4			
OMe – C′	172.5	172.7	173.0	171.9	172.7	173.0
OMe – CH_3	51.7	51.9	51.7	51.6	51.9	51.7
Others	-			-	33.6 33.0 31.1 25.88 25.79 25.5	33.2 33.1 31.6 25.94 25.7 25.4

Table 6. ^{13}C NMR of Ibu-Pro-Phe-OMe (6) in DMSO-d_6 (100 MHz, 60 mM)

	Ibu-Pro-Phe-OMe (6) (DMSO-d_6)	
	cis **δ (ppm)**	***trans*** **δ (ppm)**
Ibu – C^{α}	31.4	31.2
Ibu – C^{β}	19.4	18.8
Ibu – C^{β}	18.9	18.7
Ibu - C′	174.9	174.7
Pro – C^{α}	59.2	58.8
C^{β}	31.5	28.7
C^{γ}	21.9	24.1
C^{δ}	46.3	46.5
C′	171.78	171.73
Aro – C^{α}	53.0	53.5
C^{β}	36.2	36.7
OMe –C′	171.84	172.0
OMe –CH_3	52.0	51.7
Aromatic	137.4, 129.0, 128.15, 126.5	137.0 129.1, 128.07, 126.4

S9. ^{1}H and ^{13}C NMR Spectra

Figure 13. ^{1}H NMR of Ibu_{i-1}-Pro_{i}-Ala_{i+1}-OMe (**1**) in DMSO-d_6 (400 MHz, 10mM).

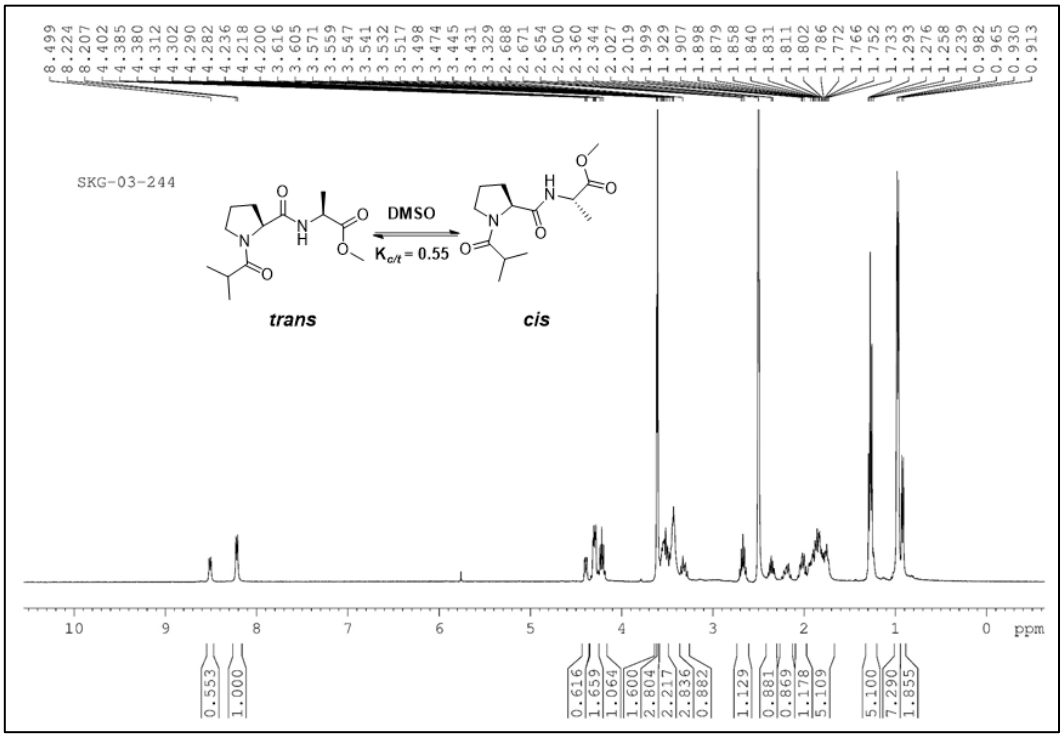

Figure 14. ^{13}C NMR of Ibu_{i-1}-Pro_{i}-Ala_{i+1}-OMe (**1**) in DMSO-d_6 (100 MHz, 60mM).

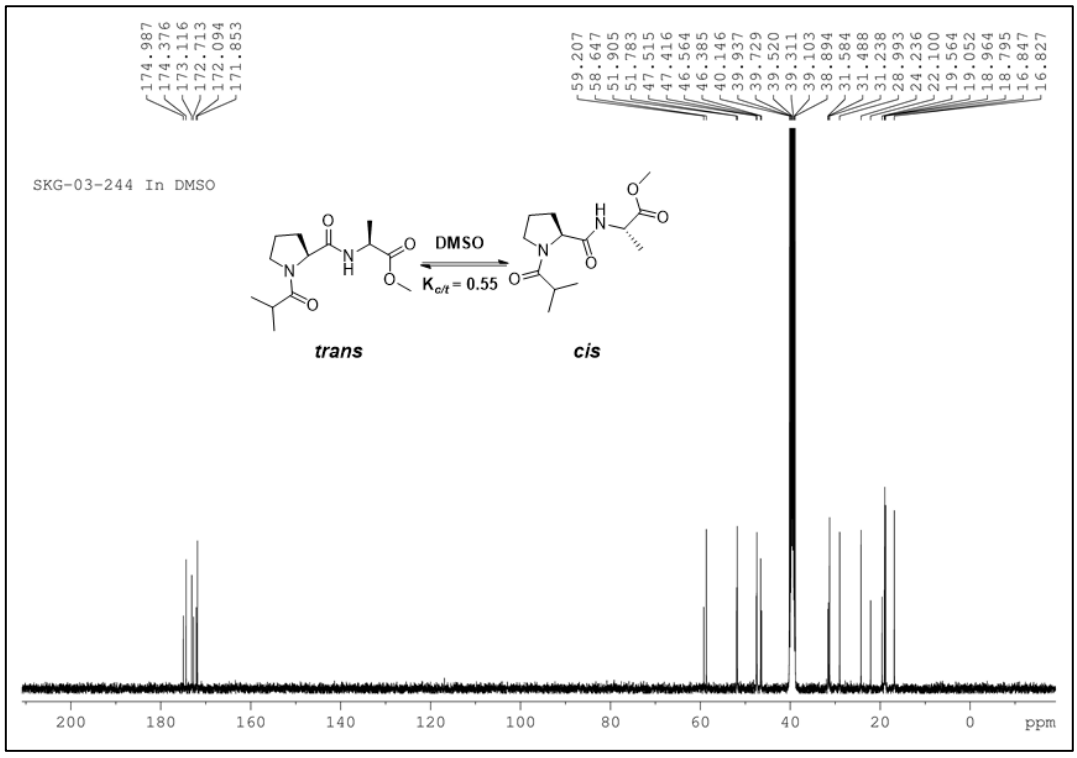

Figure 15. ^{1}H NMR of of Ibu$_{i-1}$-Pro$_{i}$-Val$_{i+1}$-OMe (**2**) in DMSO-d$_6$ (400 MHz, 10mM).

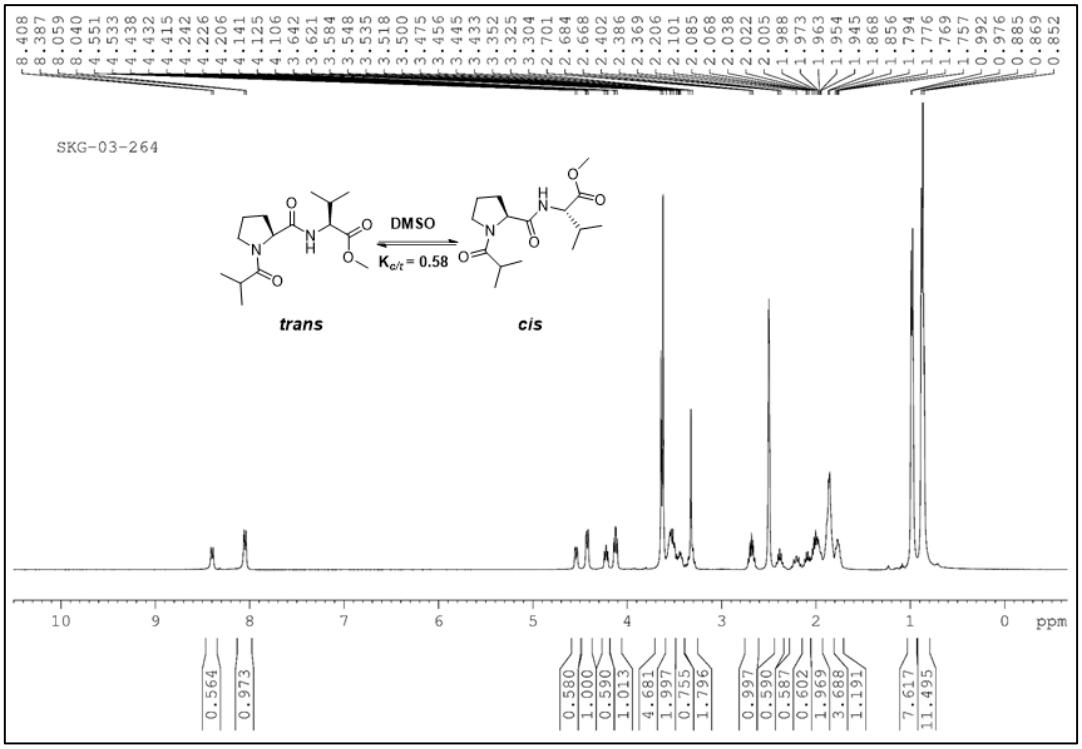

Figure 16. ^{13}C NMR of of Ibu$_{i-1}$-Pro$_{i}$-Val$_{i+1}$-OMe (**2**) in DMSO-d$_6$ (100 MHz, 60mM).

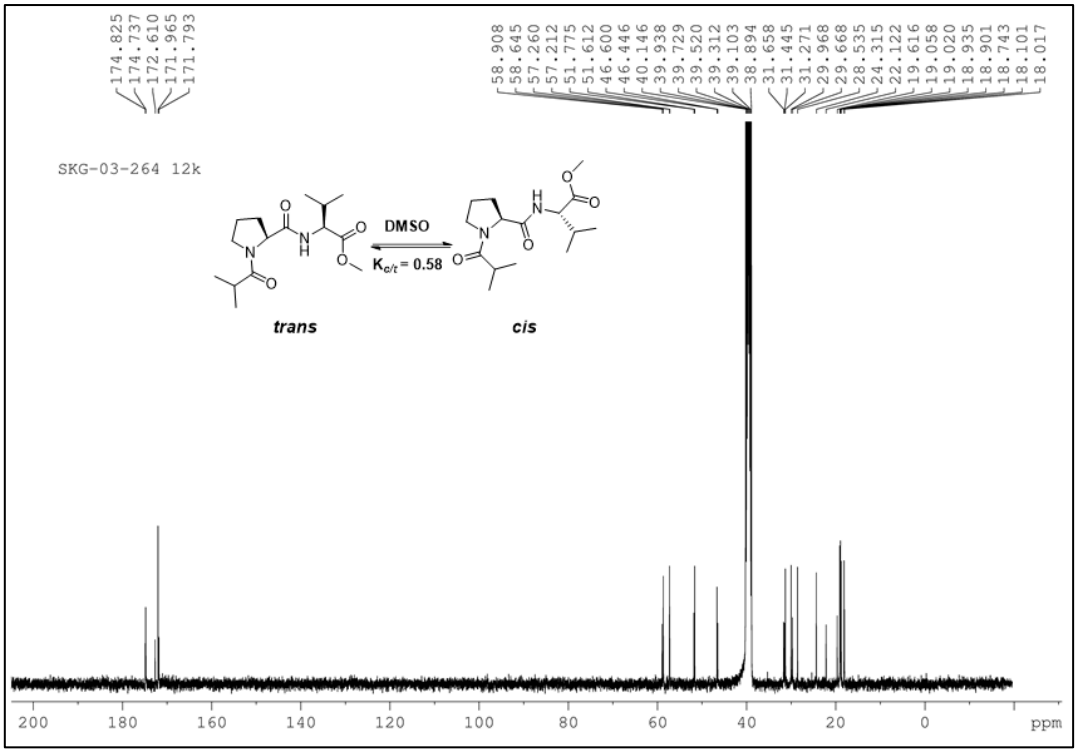

Figure 17. ^{1}H NMR of Ibu$_{i-1}$-Pro$_{i}$-Ile$_{i+1}$-OMe (**3**) in DMSO-d$_6$ (400 MHz, 10mM).

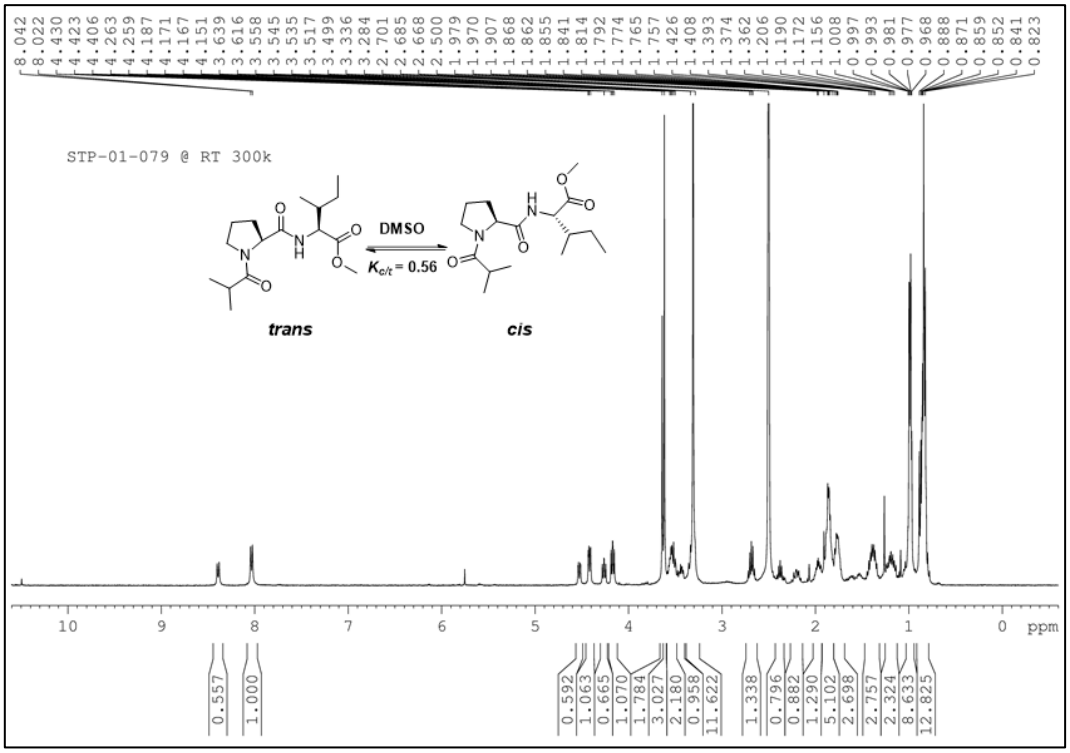

Figure 18. ^{13}C NMR of Ibu$_{i-1}$-Pro$_{i}$-Ile$_{i+1}$-OMe (**3**) in DMSO-d$_6$ (100 MHz, 60mM).

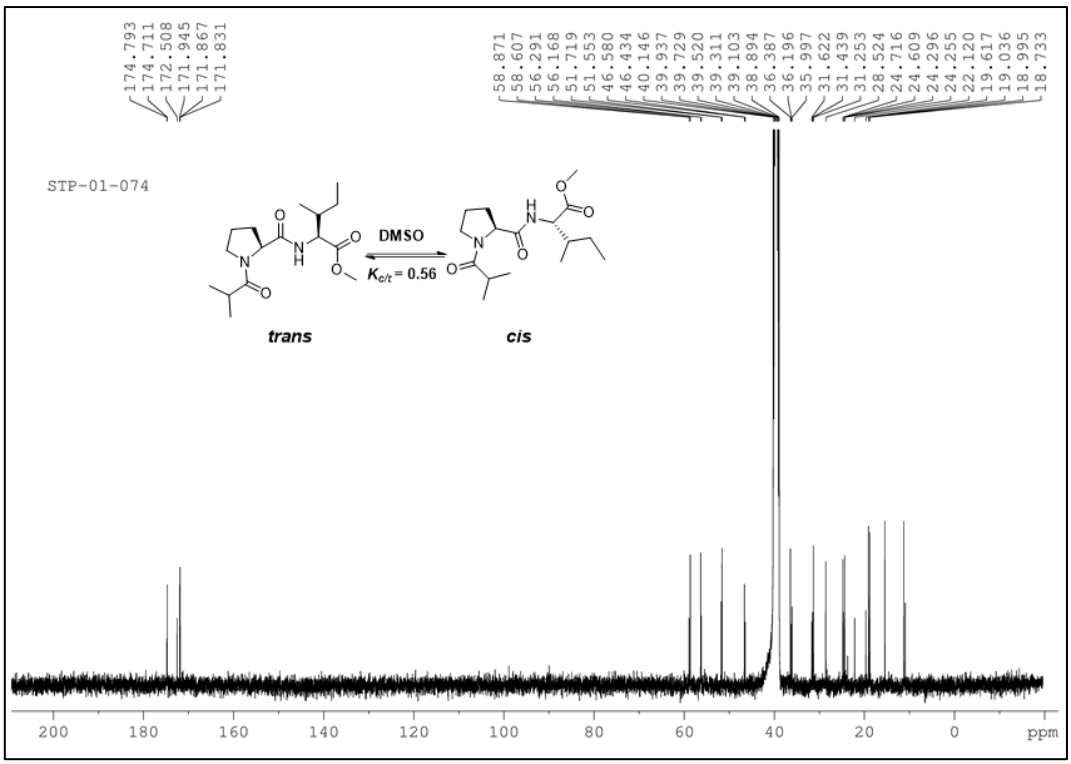

Figure 19. ^{1}H NMR of Ibu$_{i-1}$-Pro$_{i}$-Leu$_{i+1}$-OMe (**4**) in DMSO-d$_6$ (400 MHz, 10mM).

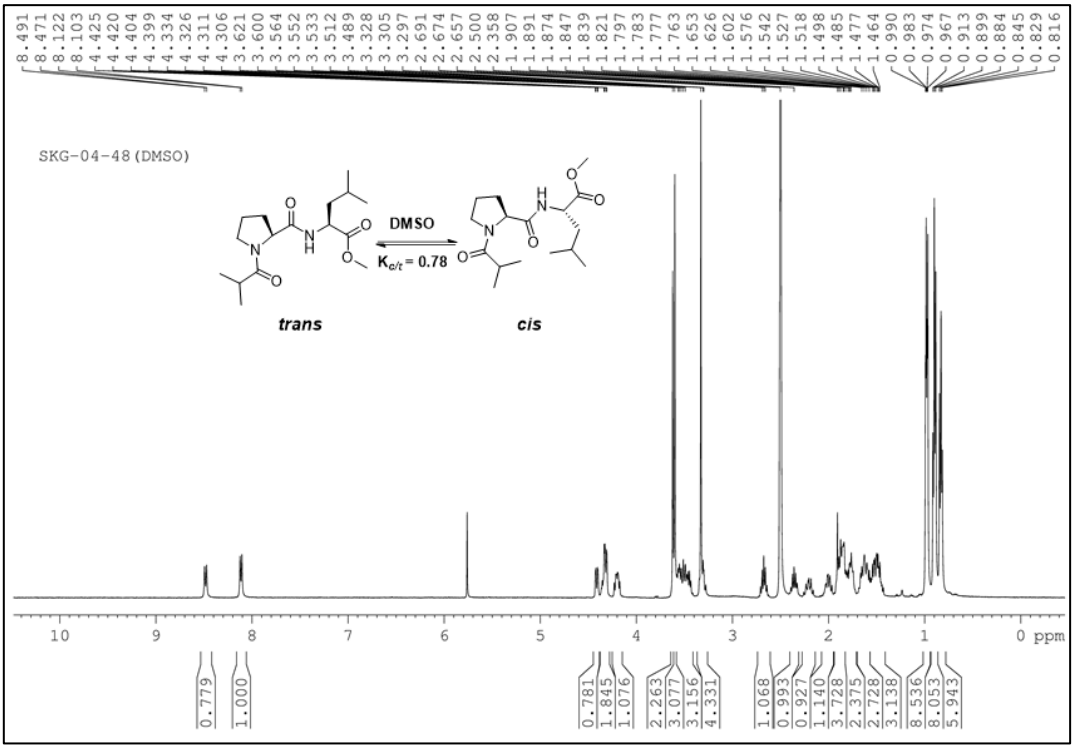

Figure 20. ^{13}C NMR of Ibu$_{i-1}$-Pro$_{i}$-Leu$_{i+1}$-OMe (**4**) in DMSO-d$_6$ (100 MHz, 60mM).

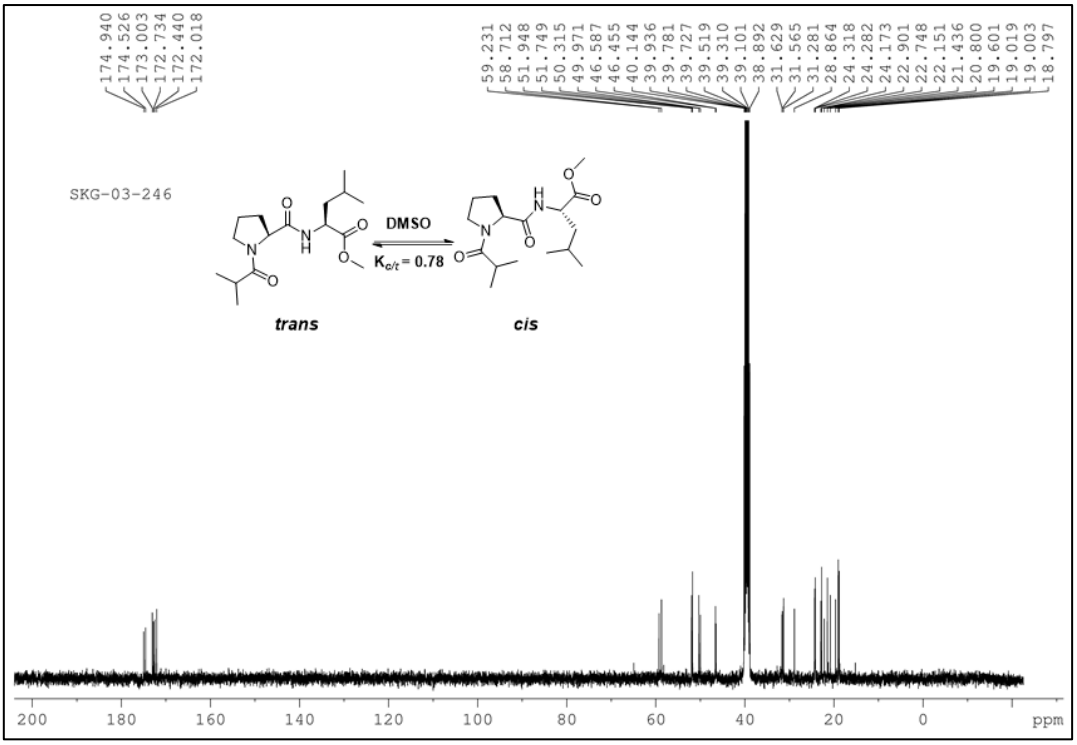

Figure 21. ^{1}H NMR of Ibu$_{i-1}$-Pro$_{i}$-Cha$_{i+1}$-OMe (**5**) in DMSO-d$_6$ (400 MHz, 10mM).

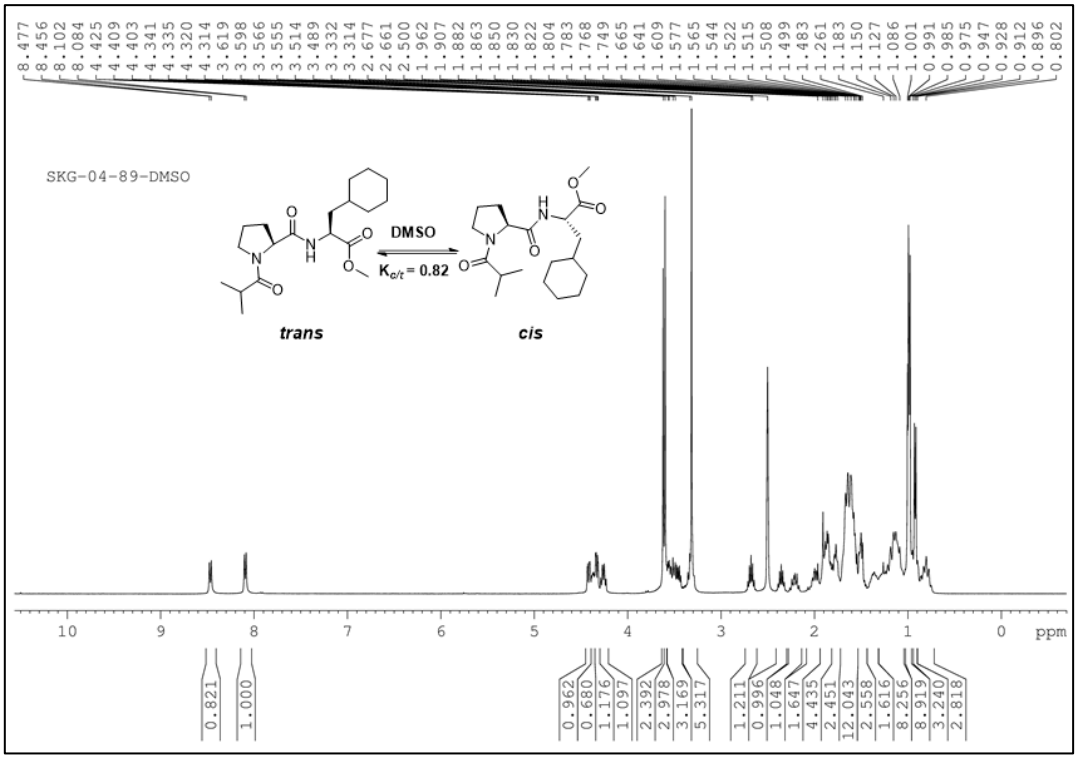

Figure 22. ^{13}C NMR of Ibu$_{i-1}$-Pro$_{i}$-Cha$_{i+1}$-OMe (**5**) in DMSO-d$_6$ (100 MHz, 60mM).

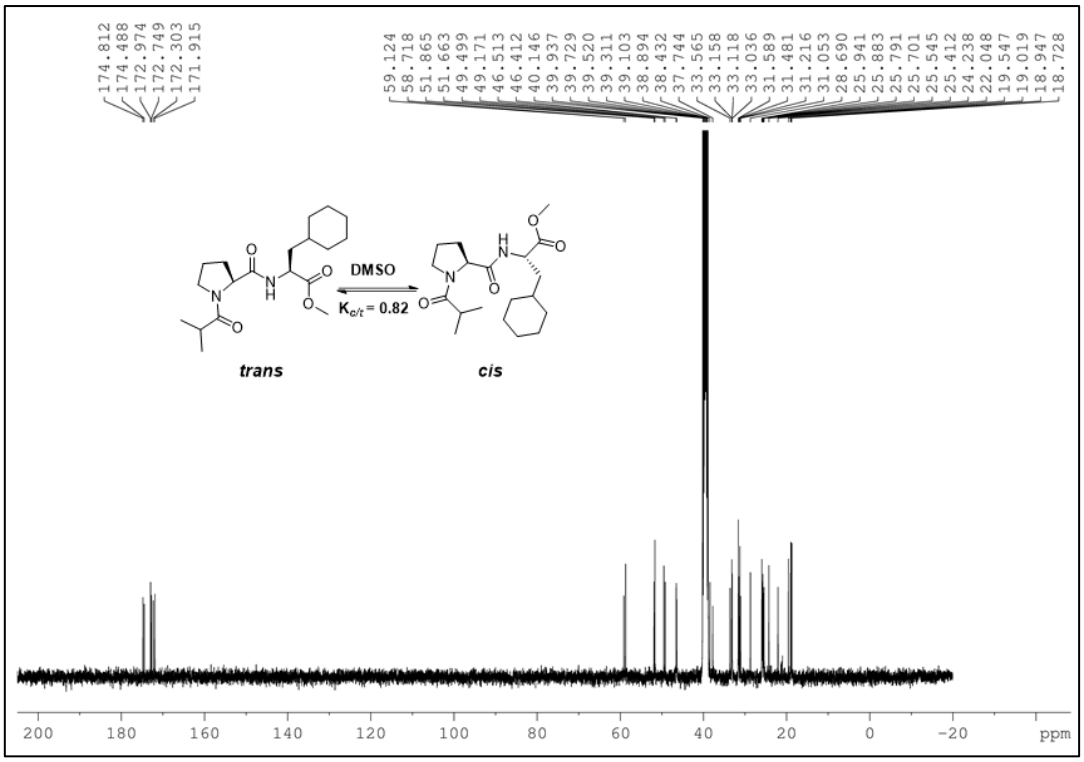

Figure 23. ^{1}H NMR of Ibu$_{i-1}$-Pro$_{i}$-Phe$_{i+1}$-OMe (**6**) in DMSO-d$_6$ (400 MHz, 10mM).

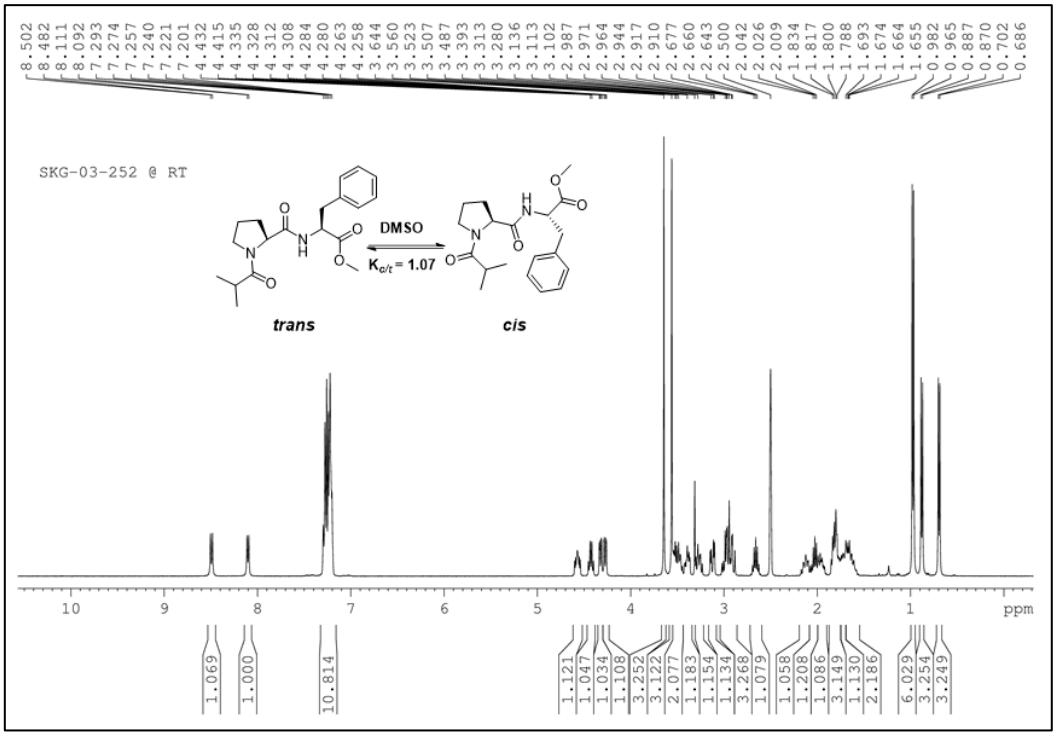

Figure 24. ^{13}C NMR of Ibu$_{i-1}$-Pro$_{i}$-Phe$_{i+1}$-OMe (**6**) in DMSO-d$_6$ (100 MHz, 60mM).

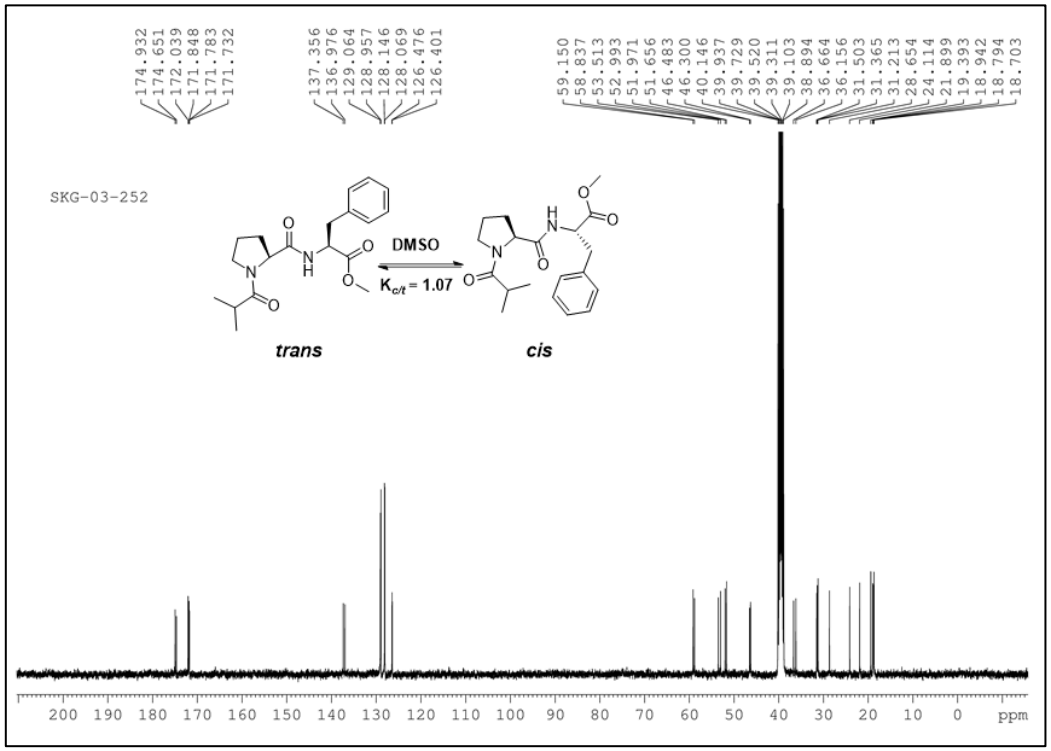

S10. Calculation of dihedral angles from ^{1}H-NMR data

Table 7.

iBu-Pro-Xaa-OMe

Xaa cis	$^{13}C_\beta$i ppm	$^{13}C_\gamma$i ppm	$\Delta\delta_{\beta\gamma}$i ppm	Ψ_{Proi} deg	$^{3}J_{N\alpha}$i+1 Hz	ϕ_{Yaa} deg	Xaa trans	$^{13}C_\beta$i ppm	$^{13}C_\gamma$i ppm	$\Delta\delta_{\beta\gamma}$i ppm	Ψ_{Proi} deg	$^{3}J_{N\alpha}$i+1 Hz	ϕ_{Yaa} deg
1	31.6	22.1	9.5	146.8	7.2	-83.8	**1**	29.0	24.2	4.8	173.1	7.2	-83.8
2	31.7	22.2	9.5	146.8	8.4	-94.7	**2**	28.5	24.3	4.2	156.4	7.6	-87.2
3	31.6	22.1	9.5	146.8	8.4	-94.7	**3**	28.5	24.3	4.2	156.4	8.4	-94.7
4	31.6	22.2	9.6	148.0	8.0	-90.8	**4**	28.9	24.2	4.7	170.3	7.2	-83.8
5	31.6	22.0	9.4	145.6	8.4	-94.7	**5**	28.7	24.2	4.5	164.7	7.2	-83.8
6	31.5	21.9	9.6	148.0	7.2	-83.8	**6**	28.7	24.1	4.6	167.5	7.6	-87.2

$\Delta\delta_{\beta\gamma} = {}^{13}C_\beta - {}^{13}C_\gamma$; $\Delta\delta_{\beta\gamma} = a\,|\theta| + b$; $\theta = (\Delta\delta_{\beta\gamma} - b) / a$; $\psi_{Pro} = \theta + 60^{o}$;

θ_{cis} : a = 0.081, b = 2.47; θ_{trans} : a = 0.036, b = 0.73;

S11. Superimposed cis and trans conformations of 1-6

Figure 25.

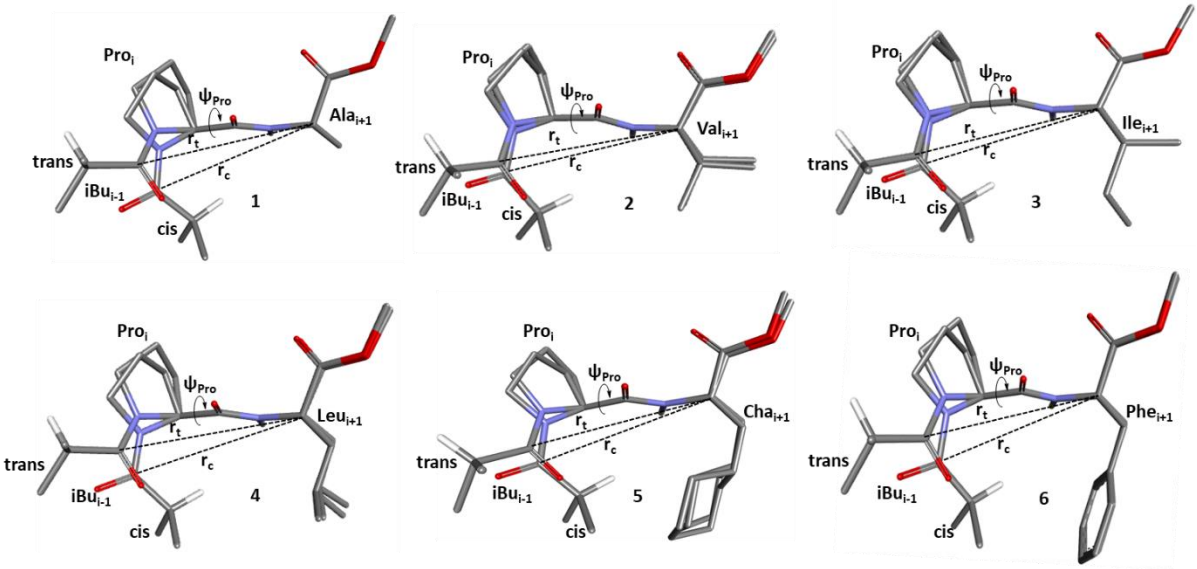

Table 8. Dihedral angles and distances in **1**-**6**

Xaa	ω_{Pro} (deg)	φ_{Pro} (deg)	ψ_{Pro} (deg)	ω_{Xaa} (deg)	φ_{Xaa} (deg)	$\chi1_{Xaa}$ (deg)	$\chi2_{Xaa}$ (deg)	r_c or r_t (Å)
1 cis	0	-71	146.8	-180	-83.8	-	-	5.317
1 trans	-180	-71	173.1	-180	-83.8	-	-	5.494
2 cis	0	-71	146.8	-180	-94.7	-62.9	-	5.317
2 trans	-180	-71	156.4	-180	-83.8	-62.9	-	5.392
3 cis	0	-71	146.8	-180	-94.7	-60	177	5.317
3 trans	-180	-71	156.4	-180	-94.7	-60	177	5.392
4 cis	0	-71	145.6	-180	-90.8	-60	-62.2	5.307
4 trans	180	-71	170.3	-180	-83.8	-60	-62.2	5.479
5 cis	0	-71	145.6	-180	-94.7	-60	-120	5.327
5 trans	180	-71	164.7	-180	-83.8	-60	120	5.447
6 cis	0	-74.9	148	-178.3	-83.8	-60	-60	5.250
6 trans	-180	-74.9	167.5	-178.3	-87.2	-60	-60	5.404

Table 9. Length (d Å), surface area (A Å²) and vdW zone of residence (V Å³) of the Alp_{i+1} side chains in **1**-**5**.

No.	Xaa	d[a] Å ($\times10^{-10}$)	A[b] Å^2 ($\times10^{-20}$)	**V[c] Å^3 ($\times$10^{-30})**	$K_{c/t}$[d]	ΔG^e kcal mol^{-1}
1	Ala	1.546	18.1	**3.9**	**0.55**	0.36
2	Val	2.582	50.6	**18.0**	**0.58**	0.32
3	Ile	2.535	48.9	**17.1**	**0.56**	0.34
4	Leu	3.905	116.0	**62.4**	**0.78**	0.15
5	Cha	5.439	224.0	**168.6**	**0.82**	0.12

[a] $C^{\alpha}_{Xaa(i+1)}\cdots C^{x}_{Xaa(i+1)}$ distance where x = β for **1**; γ for **2**, **3**; δ for **4**; ζ for **5**.
[b] Area of cone of radius d and height h: $(\pi d\times(d+\sqrt{(d^2+h^2)}))$ where d=h
[c] Quarter-sphere volume for fully extended side chain;
[d] $K_{c/t}$ = [cis] / [trans]; [e]$\Delta G = -RT \ln K_{c/t}$, 300 K.

S12. Type *α* fold and i-1…i+1 vdW interactions in Urease Accessory Protein UreF (3CXN)

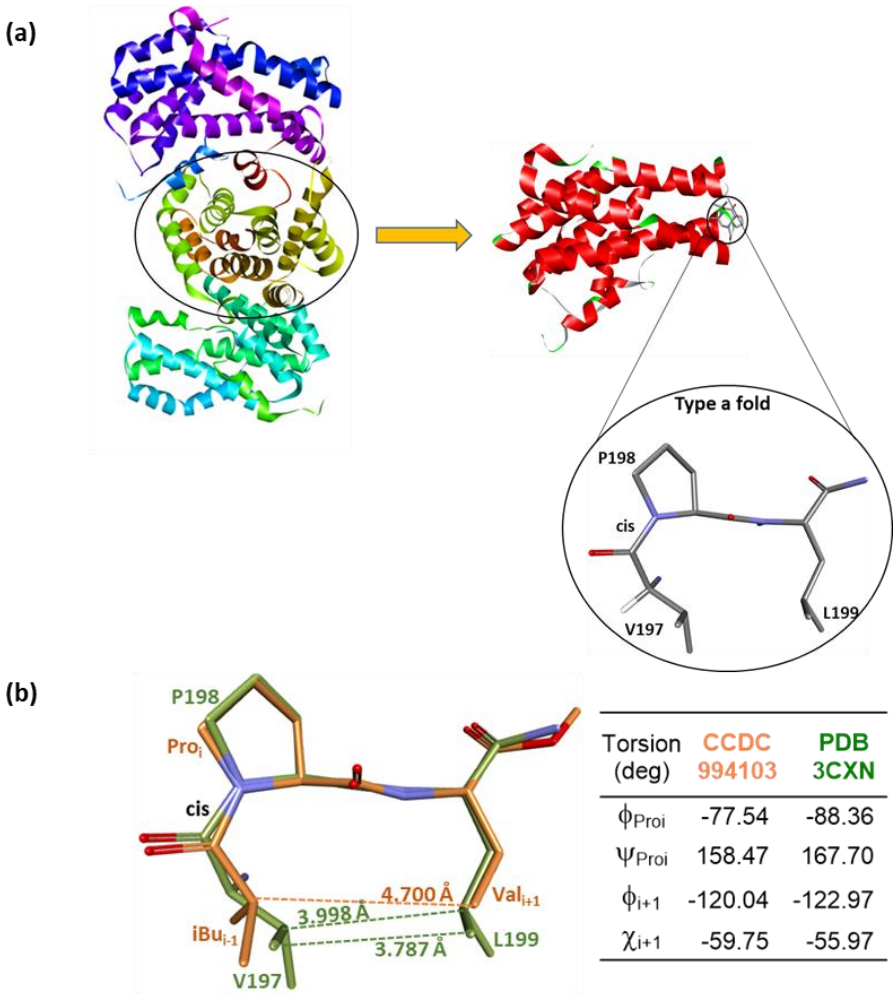

Torsion (deg)	CCDC 994103	PDB 3CXN
ϕ_{Proi}	-77.54	-88.36
Ψ_{Proi}	158.47	167.70
ϕ_{i+1}	-120.04	-122.97
χ_{i+1}	-59.75	-55.97

Figure 26. (a) PDB trimeric (multicolored, left) and the monomeric (red) structures of urease accessory protein UreF (3CXN). The type *α* fold at Val197-Pro-Leu sequence in one of the monomers (red) is highlighted. (b) Superimposed Alp-Pro-Alp segments of 3CXN (green) and crystal structure of iBu_{i-1}-Pro_i-Val_{i+1}-OMe **2** (orange) showing remarkably similar Type *α* folds. The key i-1···i+1 Alp_{i-1}···Alp_{i+1} distances and torsions are presented.